

Some Interesting Features of Memristor CNN

Makoto Itoh¹

1-19-20-203, Arae, Jonan-ku,

Fukuoka, 814-0101 JAPAN

Email: itoh-makoto@jcom.home.ne.jp

In this paper, we introduce some interesting features of a memristor CNN (Cellular Neural Network). We first show that there is the similarity between the dynamics of memristors and neurons. That is, some kind of flux-controlled memristors can *not* respond to the sinusoidal voltage source quickly, namely, they can *not* switch “on” rapidly. Furthermore, these memristors have *refractory period* after switch “on”, which means that it can *not* respond to further sinusoidal inputs until the flux is decreased. We next show that the memristor-coupled two-cell CNN can exhibit chaotic behavior. In this system, the memristors switch “off” and “on” at *irregular intervals*, and the two cells are connected when either or both of the memristors switches “on”. We then propose the modified CNN model, which can hold a binary output image, even if all cells are disconnected and no signal is supplied to the cell after a certain point of time. However, the modified CNN requires power to maintain the output image, that is, it is *volatile*. We next propose a new memristor CNN model. It can also hold a binary output state (image), even if all cells are disconnected, and no signal is supplied to the cell, by memristor’s switching behavior. Furthermore, even if we turn off the power of the system during the computation, it can resume from the previous *average* output state, since the memristor CNN has functions of both *short-term* (volatile) memory and *long-term* (non-volatile) memory. The above suspend and resume feature are useful when we want to save the current state, and continue work later from the previous state. Finally, we show that the memristor CNN can exhibit interesting two-dimensional waves, if an inductor is connected to each memristor CNN cell.

Keywords: memristor CNN; non-volatile; chaotic behavior; suspend and resume feature; long-term memory; short-term memory; two-dimensional wave; switch; neuron; synapse; excitatory; inhibitory; refractory period.

1 Introduction

In this paper, we introduce some interesting features of a memristor CNN (Cellular Neural Network).² We first study the switching behavior of flux-controlled memristors. The flux-controlled memristor switches “off” and “on”, depending on the value of the flux. Some kind of flux-controlled memristors cannot respond to the sinusoidal voltage source quickly. That is, it cannot switch “on” rapidly. Furthermore, these memristors have *refractory period* after switch “on”, that is, it can not respond to further sinusoidal inputs until the flux is decreased. We also show that the memristor-coupled two-cell can exhibit chaotic behavior. In this system, the memristors switch “off” and “on” at irregular intervals, and the two cells are connected when either or both of the memristors switches “on”.

We next propose the modified CNN and the memristor CNN. The modified CNN can hold a binary output image even if all cells are disconnected and no signal is supplied to the cell after a certain point of time. The modified CNN requires power to maintain the output image, that is, it is *volatile*. We can realize

¹After retirement from Fukuoka Institute of Technology, he has continued to study the nonlinear dynamics on memristors.

²The terminology CNN was originally used for Cellular Neural Network [1, 2]. Recently, CNN is also used for Convolutional Neural Network. In this paper, CNN stands for Cellular Neural Network.

the above switching behavior by using flux-controlled memristors, since the memristor can switch “off” and “on”, depending on the value of the flux. The memristor CNN can also hold a binary output image, even if all cells are disconnected, and even if no signal is supplied to the cell, by memristor’s switching behavior. However, it also requires power to maintain the output image, since the nonlinear element (nonlinear resistor) of the CNN cell are *volatile*.

It is well-known that the neurons can not respond to inputs quickly and they cannot generate outputs rapidly, since charging or discharging the membrane potential energy can take time. Furthermore, after firing, the neurons have *refractory period*. We show that the image processing (visual computing) of the memristor CNN can exhibit the similar behavior, if the memductance of the flux-controlled memristor has twin-peaks.

The suspend and resume feature are useful when we want to save the current state, and continue work later from the same state. We show that the memristor CNN has this kind of feature. That is, even if we turn off the power of the memristor CNN during the computation, it can recover the *average* output state later, by using the *non-volatile* memristors. Furthermore, it can resume from the previous *average* output.

In our brain’s system, a *long-term memory* is a storage system for storing and retrieving information. A *short-term memory* is the *short-time* storage system that keeps something in mind before transferring it to a long-term memory. We also show that the memristor CNN has functions of the short-term and long-term memories.

Finally, we show that the memristor CNN can exhibit interesting two-dimensional waves, if an inductor is connected to each memristor CNN cell. In this case, the dynamics of the CNN cell is given by the 2nd-order differential equation.

2 Basic Notations and Definitions

In this section, we introduce some basic notations and definitions which will be used later.

2.1 Cellular Neural Networks

Cellular Neural Network (CNN) [1, 2, 3, 4] is a dynamic nonlinear system defined by coupling only identical simple dynamical systems, called cells, located within a prescribed sphere of influence, such as nearest neighbors. The dynamics of a standard cellular neural network with a neighborhood of radius r are governed by a system of $n = MN$ differential equations

$$\begin{array}{c}
 \text{Dynamics of the CNN} \\
 \left. \begin{array}{l}
 \frac{dx_{ij}}{dt} = -\gamma x_{ij} + \sum_{k,l \in N_{ij}} (a_{kl} y_{kl} + b_{kl} u_{kl}) + z_{ij}, \\
 (i, j) \in \{1, \dots, M\} \times \{1, \dots, N\},
 \end{array} \right\} \quad (1)
 \end{array}$$

where x_{ij} , y_{kl} , u_{kl} , z_{ij} are called state, output, input, and threshold of cell C_{ij} , respectively. N_{ij} denotes the r -neighborhood of cell C_{ij} , and a_{kl} , b_{kl} , and z_{ij} denote the feedback, control, and threshold template parameters, respectively. The output y_{ij} and the state x_{ij} of each cell are usually related via the piecewise-linear saturation function

$$y_{ij} = f(x_{ij}) \triangleq \frac{1}{2} (|x_{ij} + 1| - |x_{ij} - 1|). \quad (2)$$

The matrices $A = [a_{kl}]$ and $B = [b_{kl}]$ are referred to as the feedback template A and the feedforward (input) template B , respectively. If we restrict the neighborhood radius of every cell to 1, then the cell C_{ij} is coupled only to its eight neighbor cells C_{kl} , where

$$(k, l) = (i + 1, j + 1), (i + 1, j), (i + 1, j - 1), (i, j + 1), (i, j - 1), (i - 1, j + 1), (i - 1, j), (i - 1, j - 1). \quad (3)$$

Assume that z_{ij} is the same for the whole network, that is, $z_{ij} = z$, and set $\gamma = 1$ for the sake of simplicity. Then, the template $\{A, B, z\}$ is fully specified by 19 parameters, which are the elements of two 3×3 matrices A and B , namely

$$A = \begin{array}{|c|c|c|} \hline a_{-1,-1} & a_{-1,0} & a_{-1,1} \\ \hline a_{0,-1} & a_{0,0} & a_{0,1} \\ \hline a_{1,-1} & a_{1,0} & a_{1,1} \\ \hline \end{array}, \quad B = \begin{array}{|c|c|c|} \hline b_{-1,-1} & b_{-1,0} & b_{-1,1} \\ \hline b_{0,-1} & b_{0,0} & b_{0,1} \\ \hline b_{1,-1} & b_{1,0} & b_{1,1} \\ \hline \end{array}, \quad (4)$$

and a real number z . The output and input for the cell cell C_{ij} are specified by

$$Y = \begin{array}{|c|c|c|} \hline y_{i-1,j-1} & y_{i-1,j} & y_{i-1,j+1} \\ \hline y_{i,j-1} & y_{i,j} & y_{i,j+1} \\ \hline y_{i+1,j-1} & y_{i+1,j} & y_{i+1,j+1} \\ \hline \end{array}, \quad (5)$$

$$U = \begin{array}{|c|c|c|} \hline u_{i-1,j-1} & u_{i-1,j} & u_{i-1,j} \\ \hline u_{i,j-1} & u_{i,j} & u_{i,j+1} \\ \hline u_{i+1,j-1} & u_{i+1,j} & u_{i+1,j+1} \\ \hline \end{array}.$$

Here, we assumed that the feedback parameters a_{kl} and the control template parameters b_{kl} do not vary with space, that is, they can be defined as [1, 2]

$$a_{kl} \triangleq a_{k-i, l-j}, \quad b_{kl} \triangleq b_{k-i, l-j}. \quad (6)$$

For example,

$$\left. \begin{array}{ll} \text{if } k = i, l = j, & \text{then } \begin{array}{l} a_{kl} = a_{k-i, l-j} = a_{0,0} \\ b_{kl} = b_{k-i, l-j} = b_{0,0} \end{array} \end{array} \right\} \quad (7)$$

$$\left. \begin{array}{ll} \text{if } k = i, l = j + 1, & \text{then } \begin{array}{l} a_{kl} = a_{k-i, l-j} = a_{0,1} \\ b_{kl} = b_{k-i, l-j} = b_{0,1} \end{array} \end{array} \right\}$$

Thus, we obtained the four elements:

$$a_{0,0}, a_{0,1}, b_{0,0}, b_{0,1}, \quad (8)$$

in Eq. (4). Similarly, we can obtain all other elements of templates A and B .

The CNN template $\{A, B, z\}$ is usually designed such that the qualitative behavior is not affected by the small perturbation of the template. If the CNN template satisfies this property, then the output image remains unchanged, even if we change the template parameters slightly. It also remains unchanged in the presence of sufficiently small noise.

Many applications of the CNN templates are to convert gray-scale images to binary images. In this paper, the luminance value of the pixel would be coded as black $\rightarrow +1$, white $\rightarrow -1$, gray $\rightarrow (-1, 1)$. Furthermore, in order to simulate Eq. (1) in a computer, the initial condition $x_{ij}(0)$ and the boundary condition must be specified. For example, the fixed boundary condition is given by

$$v_{k^*l^*} = v_0, \quad u_{k^*l^*} = u_0, \quad (9)$$

where k^*l^* denotes boundary cells, and v_0 and u_0 are constants.

Finally, let us consider an isolated CNN cell, which does not have the inputs, the outputs from other cells, and the threshold, for later use. Its dynamics is given by the first-order differential equation:

$$\begin{aligned} \frac{dx_{ij}}{dt} &= -x_{ij} + a_{0,0} y_{ij} = -x_{ij} + a_{0,0} f(x_{ij}) \\ &= -x_{ij} + \frac{a_{0,0}}{2} (|x_{ij} + 1| - |x_{ij} - 1|), \end{aligned} \quad (10)$$

where $a_{0,0}$ is the feedback parameter. The output y_{ij} and the state x_{ij} of the isolated cell C_{ij} is related by

$$y_{ij} = f(x_{ij}) \triangleq \frac{1}{2} (|x_{ij} + 1| - |x_{ij} - 1|). \quad (11)$$

Assume $a_{0,0} > 1$. Then Eq. (10) has three equilibrium points, one is unstable and others are stable [1]. We study its detailed behavior in Sec. 4.1.

2.2 Memristors

The *memristor* shown in Figures 1-3 is a passive 2-terminal electronic device described by a nonlinear relation

$$\varphi = g(q), \quad \text{or} \quad q = h(\varphi), \quad (12)$$

between the charge q and the flux φ [5, 6]. Its terminal voltage v and the terminal current i is given by

$v - i$ characteristic of memristors

$$v = M(q)i, \quad \text{or} \quad i = W(\varphi)v, \quad (13)$$

where

$$v = \frac{d\varphi}{dt}, \quad \text{and} \quad i = \frac{dq}{dt}. \quad (14)$$

The two nonlinear functions $M(q)$ and $W(\varphi)$, called the *memristance* and *memductance*, respectively, are defined by

$$M(q) \triangleq \frac{dg(q)}{dq}, \quad (15)$$

and

$$W(\varphi) \triangleq \frac{dh(\varphi)}{d\varphi}, \quad (16)$$

representing the *slope* of a scalar function $\varphi = \varphi(q)$ and $q = q(\varphi)$, respectively, called the *memristor constitutive relation*.

A memristor characterized by a differentiable $q - \varphi$ (resp., $\varphi - q$) characteristic curve is *passive* if, and only if, its small-signal memristance $M(q)$ (resp., small-signal memductance $W(\varphi)$) is nonnegative (see [5]). Since the instantaneous power dissipated by the above memristor is given by

$$p(t) = M(q(t)) i(t)^2 \geq 0, \quad (17)$$

or

$$p(t) = W(\varphi(t)) v(t)^2 \geq 0, \quad (18)$$

the energy flow into the memristor from time t_0 to t satisfies

$$\int_{t_0}^t p(\tau) d\tau \geq 0, \quad (19)$$

for all $t \geq t_0$.

In this paper, we assume the followings unless otherwise noted:

1. The memristor is *ideal*, that is, it is endowed with a *nonvolatility property*.
2. The *passive* memristor will not lose its flux or charge via the parasitic elements when we switch off the power.

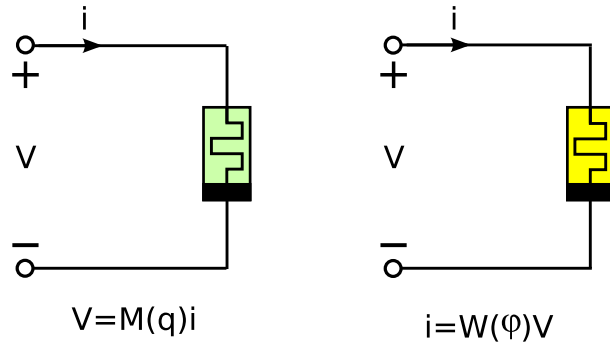


Figure 1: $v-i$ characteristic of memristors: charge-controlled memristor with the terminal voltage $v = M(q) i$ (left). flux-controlled memristor with the terminal current $i = W(\varphi) v$ (right).

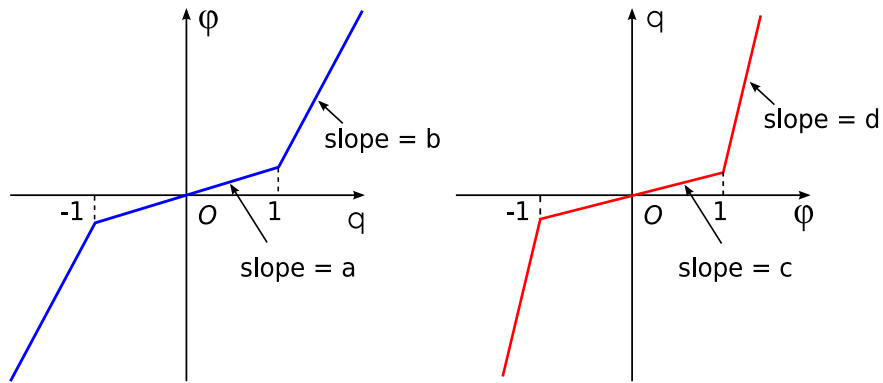


Figure 2: The constitutive relation of a monotone-increasing piecewise-linear memristor: charge-controlled memristor described by a nonlinear relation $\varphi = g(q) \triangleq bq + 0.5(a-b)(|q+1| - |q-1|)$ (left). flux-controlled memristor described by a nonlinear relation $q = h(\varphi) \triangleq c\varphi + 0.5(c-d)(|\varphi+1| - |\varphi-1|)$ (right).

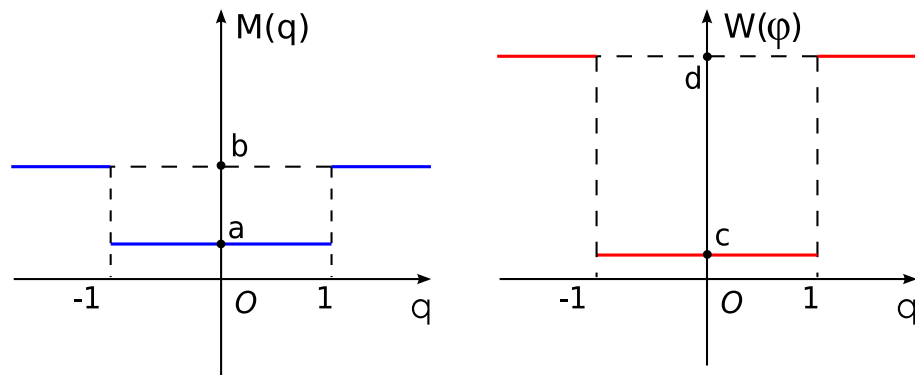


Figure 3: Memristance $M(q)$ of a charge-controlled memristor (left). Memductance $W(\varphi)$ of a flux-controlled memristor (right).

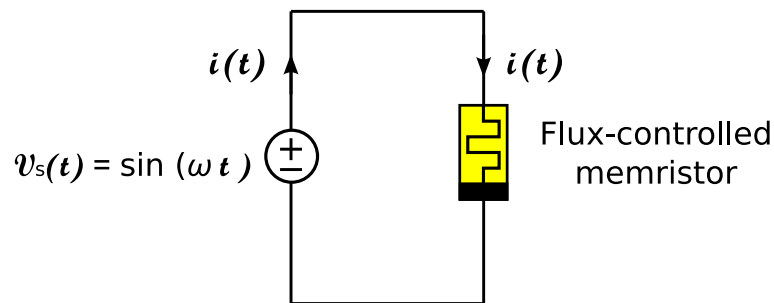


Figure 4: Two-element circuit which consists of a flux-controlled memristor and a periodic voltage source $v_s(t) = \sin(\omega t)$, where $\omega = 0.2$.

3 Neuron-like Response of Memristors

Consider the two-element circuit shown in Figure 4. It consists of a flux-controlled memristor and a periodic voltage source $v_s(t) = \sin(\omega t)$, where $\omega = 0.2$. The constitutive relation of the flux-controlled memristor is given by

$$q = h(\varphi) = 0.5 (|\varphi - a| - |\varphi - b| + b - a), \quad (20)$$

where $a = 0.5$, $b = 7$ (see Figure 5(a)), and the flux $\varphi(t)$ is defined by

$$\varphi(t) = \int_{-\infty}^t v_s(\tau) d\tau. \quad (21)$$

The memductance $W(\varphi)$ is given by

$$\begin{aligned} W(\varphi) &= \frac{dh(\varphi)}{d\varphi} = \mathfrak{s}[\varphi + 0.5] - \mathfrak{s}[\varphi - 7] \\ &= \begin{cases} 1 & \text{for } 0.5 < \varphi < 7, \\ 0 & \text{for } \varphi \leq 0.5 \text{ and } \varphi \geq 7, \end{cases} \end{aligned} \quad (22)$$

where $\mathfrak{s}[z]$ denotes the *unit step* function, equal to 0 for $z < 0$ and 1 for $z \geq 0$. Thus, the memristor switches “off” and “on”, depending on the value of the flux φ as shown in Figure 5(b). Its terminal voltage $v(t)$ and the terminal current $i(t)$ satisfy

$$i(t) = W(\varphi(t)) v_s(t), \quad (23)$$

where

$$\frac{d\varphi(t)}{dt} = v(t) = v_s(t) = \sin(\omega t). \quad (24)$$

We show the pinched hysteresis loop of flux-controlled memristor in Figure 6. We also show the waveforms of the terminal voltage $v(t)$, the terminal current $i(t)$, the flux $\varphi(t)$, and the memductance $W(\varphi(t))$ in Figure 7. Observe that the current flows through the memristor if $0.5 < \varphi(t) < 7$ and no current flows through the memristor if $\varphi \leq 0.5$ and $\varphi \geq 7$ as shown in Figure 7(c), since the memristor switches “off” and “on”, depending on the value of the flux φ as shown in Figure 7(c).

There is the similarity between memristors and neurons. That is, the neurons cannot respond to inputs quickly and they cannot generate outputs rapidly. Charging or discharging the membrane potential energy can take time. Furthermore, after firing, the neurons have *refractory period* (the period during which the neurons can not respond to further stimulation). Thus, we conclude as follow:

The flux-controlled memristor defined by Eq. (23) cannot respond to the sinusoidal voltage source $v_s(t) = \sin(0.2t)$ quickly. That is, it cannot switch “on” rapidly. Furthermore, this memristor has *refractory period* after switch “on”, that is, it can not respond to further sinusoidal inputs until the flux is decreased.

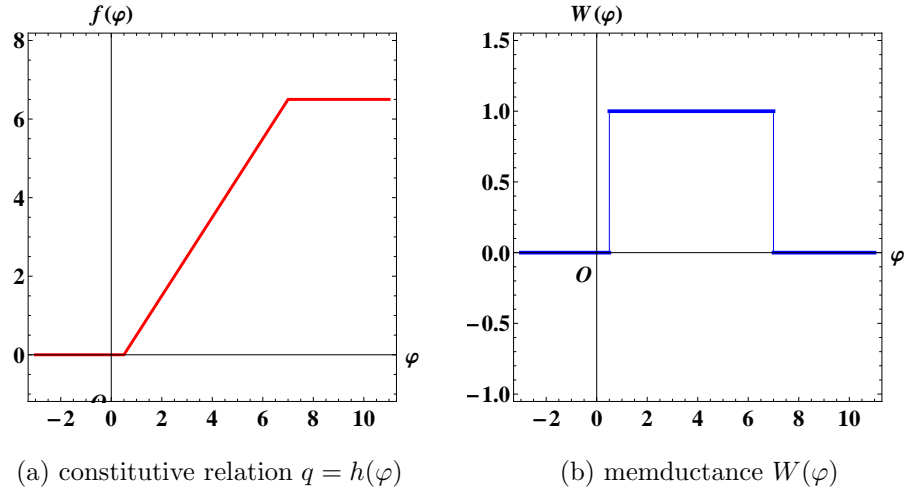


Figure 5: Characteristic of the flux-controlled memristor. The memristor switches off and on depending on the value of the flux φ as shown in Figure 5(b). That is, $W(\varphi) = 0$ implies that the memristor switches off, and $W(\varphi) = 1$ implies that the memristor switches on.

- (a) The constitutive relation of the memristor, which is given by $q = h(\varphi) \triangleq 0.5(|\varphi - 0.5| - |\varphi - 7| + 6.5)$.
- (b) Memductance $W(\varphi)$ of the memristor, which is defined by $W(\varphi) \triangleq \frac{dh(\varphi)}{d\varphi}$. Thus, $W(\varphi) = 1$ for $0.5 < \varphi < 7$, and $W(\varphi) = 0$ for $\varphi \leq 0.5$ and $\varphi \geq 7$.

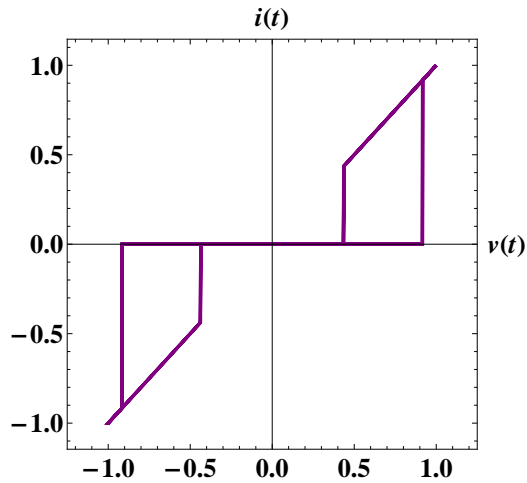
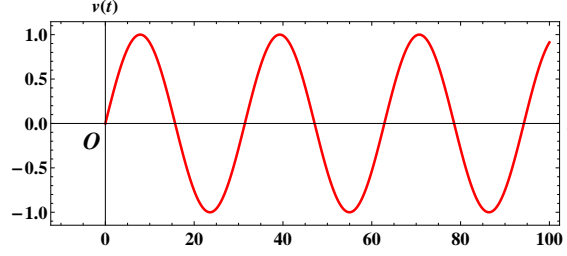
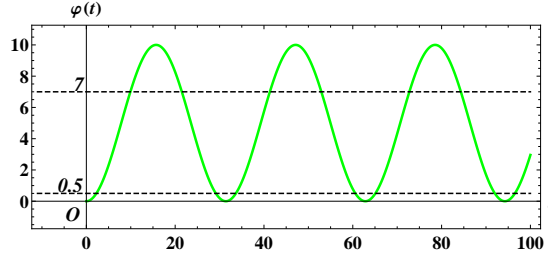


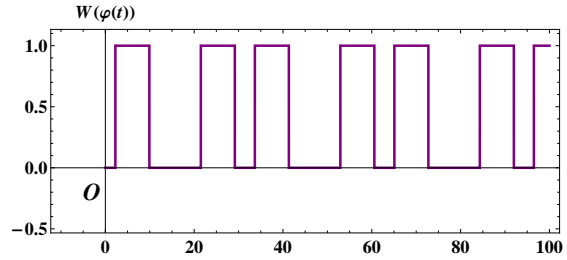
Figure 6: Pinched hysteresis loop driven by a periodic voltage source $v_s(t) = \sin(\omega t)$, where $\omega = 0.2$.



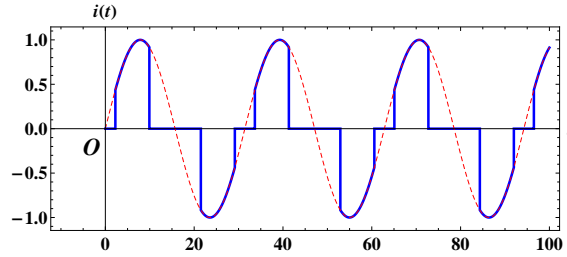
(a) driving source $v_s(t)$



(b) flux $\varphi(t)$



(c) memductance $W(\varphi(t))$



(d) current $i(t)$

Figure 7: Waveforms of the flux-controlled memristor. The memristor switches “off” and “on”, depending on the value of the flux φ as shown in Figure 7(c). The current $i(t)$ flows through the memristor if $0.5 < \varphi(t) < 7$, and no current flows through the memristor if $\varphi \leq 0.5$ or $\varphi \geq 7$ as shown in Figure 7(d). Initial condition of Eq. (24): $\varphi(0) = 0$.

(a) Waveform of the driving source $v_s(t)$, which is defined by $v_s(t) = \sin(\omega t)$, where $\omega = 0.2$.

(b) Waveform of the flux $\varphi(t)$ across the memristor, which is defined by $\varphi(t) = \int_0^t v_s(\tau) d\tau$.

(c) Waveform of the memductance $W(\varphi(t))$, which is defined by $W(\varphi) = \mathfrak{s}[\varphi + 0.5] - \mathfrak{s}[\varphi - 7]$.

(d) Waveform of the current $i(t)$ through the memristor, which is defined by $i(t) = W(\varphi)v_s(t)$ (blue). Red dashed line denotes the waveform of the driving source $v_s(t)$.

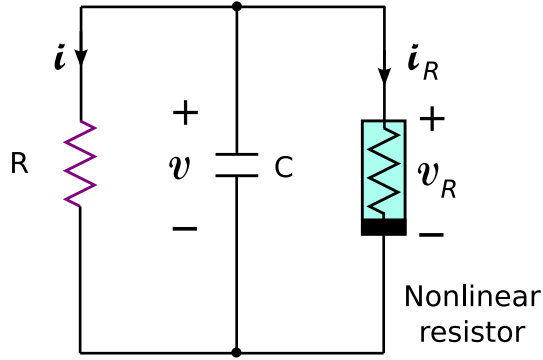


Figure 8: Isolated CNN cell which consists of a linear resistor, linear capacitor, and a nonlinear resistor. Parameters: $R = 1$, $C = 1$, $i_R = f_R(v_R) \triangleq -0.5a(|v_R + 1| - |v_R - 1|)$, where a is a constant.

4 Chaotic Oscillation from Memristor-Coupled CNNs

It is well known that an *autonomous* two-cell CNN exhibits a limit cycle, and a second-order *non-autonomous* CNN exhibits a chaotic attractor [1, 2]. In this paper, we show that a non-autonomous *memristor-coupled* CNN can also exhibit a chaotic attractor.

4.1 Isolated CNN cell

An isolated CNN cell, without the inputs, the outputs from other cells, and the threshold, can be realized by the circuit in Figure 8. The dynamics of this circuit is given by

$$C \frac{dv}{dt} = -\frac{v}{R} - f_R(v_R), \quad (25)$$

where $R = 1$, $C = 1$, $v_R = v$. The characteristic of the nonlinear resistor is given by

$$i_R = f_R(v_R) = -0.5a(|v_R + 1| - |v_R - 1|), \quad (26)$$

where a is a constant. If $a > 0$, then the nonlinear resistor is active as shown in Figure 9. Substituting Eq. (26) into Eq. (25), we obtain

$$\frac{dv}{dt} = F(v) \triangleq -v + 0.5a(|v + 1| - |v - 1|). \quad (27)$$

If $a > 1$, then Eq. (27) has three equilibrium points. The two equilibrium points are located on both sides of the origin, and they are stable. The other one is the origin O , which is unstable. For example, if $a = 2$, then the equilibrium points P_1 ($v = -2$) and P_2 ($v = 2$) are stable and the origin is unstable, as shown in Figure 10. Thus, we obtain

$$\begin{cases} \text{if } v(0) < 0 & \lim_{t \rightarrow \infty} v(t) \rightarrow -2, \\ \text{if } v(0) > 0 & \lim_{t \rightarrow \infty} v(t) \rightarrow 2, \\ \text{if } v(0) = 0 & v(t) = 0 \text{ for all } t > 0. \end{cases} \quad (28)$$

The above behavior will be used in Sec. 5.

Equations (25) and (27) can be recast into the well-known first-order equation of the standard isolated CNN cell

Dynamics of isolated CNN cell

$$\frac{dv}{dt} = -v + a_{0,0} f(v), \quad (29)$$

where $a_{0,0} = a$ and $f(v) = 0.5(|v + 1| - |v - 1|)$ (see Eq. (10)).

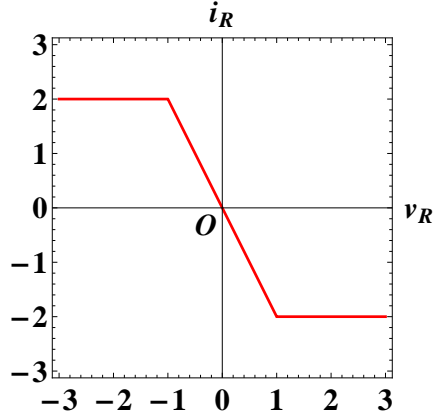


Figure 9: $v - i$ characteristic of the nonlinear resistor, which is defined by $i_R = f_R(v_R) \triangleq -0.5 a (|v_R + 1| - |v_R - 1|)$, where $a = 2$.

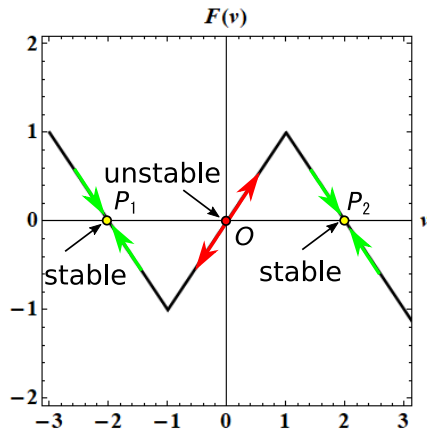


Figure 10: Driving-point plot of Eq. (27) with $a = 2$. Equation(27) has two stable equilibrium points $v = \pm 2$ (yellow), and the origin $v = 0$ (red) is unstable.

4.2 Non-autonomous two-cell CNNs

Let us consider the *non-autonomous* two-cell CNN in Figure 11 [1]. It is driven by an independent current source. The dynamics of the circuit is given by

$$\left. \begin{aligned} C \frac{dv_1}{dt} &= -\frac{v_1}{R} - g(v_1) - h(v_2) + j(t), \\ C \frac{dv_2}{dt} &= -\frac{v_2}{R} - g(v_2) + h(v_1), \end{aligned} \right\} \quad (30)$$

where

$$\left. \begin{aligned} R &= 1, \quad C = 1, \\ j(t) &= 4.04 \sin\left(\frac{\pi}{2}t\right), \\ g(x) &= -(|x+1| - |x-1|), \\ h(x) &= 0.6(|x+1| - |x-1|). \end{aligned} \right\} \quad (31)$$

In this circuit, the two nonlinear resistors have the same current-voltage characteristics, that is,

$$\left. \begin{aligned} i_R &= g(v_R) = -(|v_R+1| - |v_R-1|), \\ i_r &= g(v_r) = -(|v_r+1| - |v_r-1|). \end{aligned} \right\} \quad (32)$$

The two voltage-controlled current sources are defined by

$$\left. \begin{aligned} i_3 &= -h(v_2) = -0.6(|v_2+1| - |v_2-1|), \\ i_4 &= h(v_1) = 0.6(|v_1+1| - |v_1-1|). \end{aligned} \right\} \quad (33)$$

Equation (30) is recast into the second-order non-autonomous CNN equation [1]:

$$\left(\begin{array}{l} \text{Dynamics of non-autonomous CNN} \\ \\ \frac{dv_1}{dt} = -v_1 + a_{0,0}f(v_1) + a_{0,1}f(v_2) + j(t), \\ \frac{dv_2}{dt} = -v_2 + a_{0,-1}f(v_1) + a_{0,0}f(v_2), \end{array} \right) \quad (34)$$

where $a_{0,0} = 2$, $a_{0,-1} = -a_{0,1} = 1.2$, and

$$f(x) = 0.5(|x+1| - |x-1|). \quad (35)$$

We show the well-known chaotic trajectory and the associated Poincaré map of Eq. (30) in Figure 12 [1].

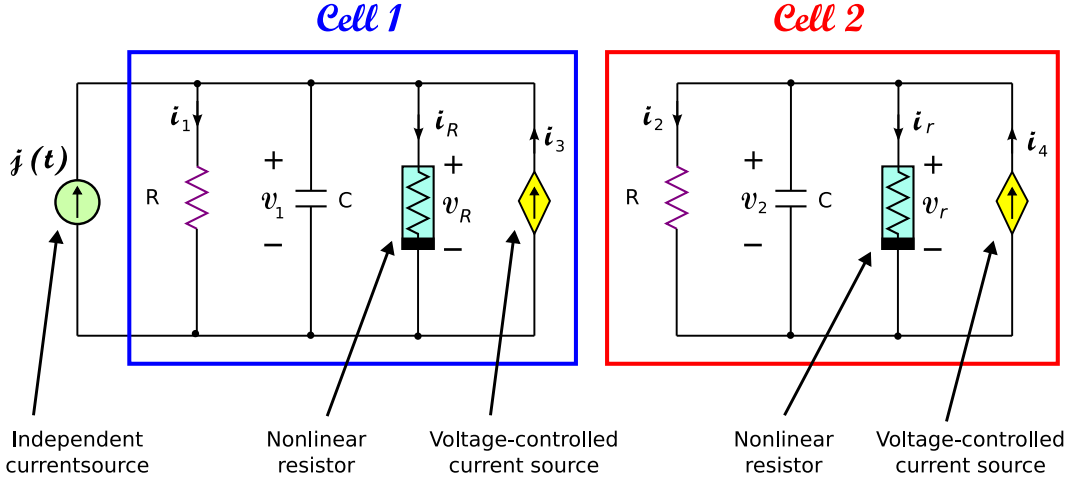
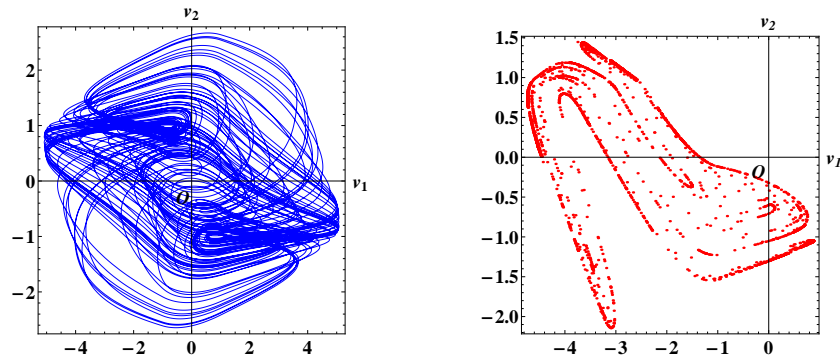


Figure 11: Two-cell CNN with an independent current source $j(t) = 4.04 \sin(\frac{\pi}{2}t)$. Parameters: $R = 1$, $C = 1$.

(1) The two nonlinear resistors (cyan) have the same current-voltage characteristics: $i_R = g(v_R) \triangleq -(|v_R + 1| - |v_R - 1|)$ (left) and $i_r = g(v_r) \triangleq -(|v_r + 1| - |v_r - 1|)$ (right).

(2) The two voltage-controlled current sources (yellow) are defined by $i_3 = -h(v_2) \triangleq -0.6(|v_2 + 1| - |v_2 - 1|)$ (left) and $i_4 = h(v_1) \triangleq 0.6(|v_1 + 1| - |v_1 - 1|)$ (right).



(a) Chaotic trajectory on the (v_1, v_2) -plane (b) Associated Poincaré map

Figure 12: Chaotic trajectory of Eq. (30) and associated Poincaré map. The attractor in Figure 12(b) is called the “Lady’s shoe attractor”. Initial condition: $v_1(0) = 0$, $v_2 = 0$.

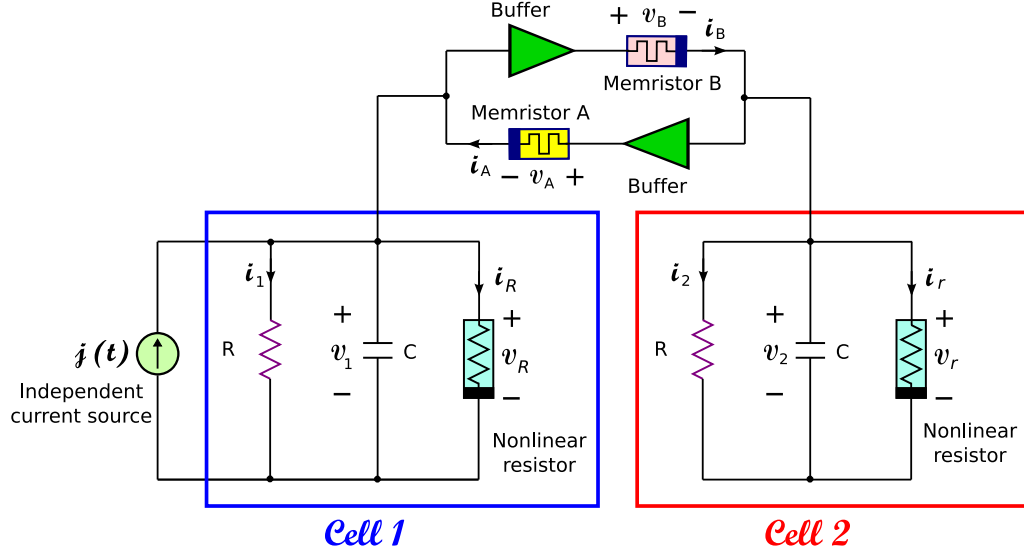


Figure 13: Two-cell CNN which is coupled with flux-controlled memristors.

(1) Parameters: $R = 1$, $C = 1$.

(2) The cell 1 (left) is driven by an independent current source (light-green): $j(t) = 4 \sin\left(\frac{2\pi}{3}t\right)$.

(3) The memristor A (yellow) is passive, while the memristor B (pink) is active.

(4) The terminal currents and voltages of the memristor A and the memristor B satisfy $i_A = W_A(\varphi_A) v_A = W_A(\varphi_A)(v_2 - v_1)$ and $i_B = W_B(\varphi_B) v_B = W_B(\varphi_B)(v_1 - v_2)$, respectively, where $\frac{d\varphi_A}{dt} = v_A = v_2 - v_1$,

$\frac{d\varphi_B}{dt} = v_B = v_1 - v_2$, $W_A(\varphi_A) = -1.2(\mathfrak{s}[\varphi_A + 2] - \mathfrak{s}[\varphi_A - 2])$, and $W_B(\varphi_B) = 1.2(\mathfrak{s}[\varphi_B + 2] + \mathfrak{s}[\varphi_B - 2])$.

The symbol $\mathfrak{s}[z]$ denotes the *unit step* function, equal to 0 for $z < 0$ and 1 for $z \geq 0$.

(5) The two nonlinear resistors (cyan) have the same current-voltage characteristics, that is, $i_R = g(v_R) \triangleq -(|v_R + 1| - |v_R - 1|)$ and $i_r = g(v_r) \triangleq -(|v_r + 1| - |v_r - 1|)$.

(6) The buffer (dark green) is a op-amp circuit which has a voltage gain of 1, that is, the output voltage is the same as the input voltage. It offers input-output isolation.

4.3 Memristor-coupled two-cell CNNs

Let us consider the non-autonomous CNN in Figure 13, whose cells are coupled with memristors. The dynamics of the circuit in Figure 13 is given by

$$\left. \begin{aligned} C \frac{dv_1}{dt} &= -\frac{v_1}{R} + g(v_1) + W_A(\varphi_A)(v_2 - v_1) + j(t), \\ C \frac{dv_2}{dt} &= -\frac{v_2}{R} + g(v_2) + W_B(\varphi_B)(v_1 - v_2), \\ \frac{d\varphi_A}{dt} &= v_A = v_2 - v_1, \\ \frac{d\varphi_B}{dt} &= v_B = v_1 - v_2, \end{aligned} \right\} \quad (36)$$

where

$$\left. \begin{aligned}
 R &= 1, C = 1, \\
 j(t) &= 4 \sin\left(\frac{2\pi}{3}t\right), \\
 g(x) &= -(|x+1| - |x-1|), \\
 W_A(\varphi_A) &= -1.2 (\mathfrak{s}[\varphi_A + 2] - \mathfrak{s}[\varphi_A - 2]) \\
 &= \begin{cases} -1.2 & \text{for } -2 \leq \varphi_A < 2, \\ 0 & \text{for } \varphi_A < -2 \text{ and } 2 \leq \varphi_A, \end{cases} \\
 W_B(\varphi_B) &= 1.2 (\mathfrak{s}[\varphi_B + 2] - \mathfrak{s}[\varphi_B - 2]) \\
 &= \begin{cases} 1.2 & \text{for } -2 \leq \varphi_B < 2, \\ 0 & \text{for } \varphi_B < -2 \text{ and } 2 \leq \varphi_B. \end{cases}
 \end{aligned} \right\} \quad (37)$$

Here, φ_A and φ_B denote the flux of the memristors A and B , respectively, $W_A(\varphi_A)$ and $W_B(\varphi_B)$ denote the memductances of the memristors A and B , respectively, $j(t)$ denotes an independent current source, and $\mathfrak{s}[z]$ denotes the *unit step* function, equal to 0 for $z < 0$ and 1 for $z \geq 0$. The two nonlinear resistors have the same current-voltage characteristics, that is,

$$\begin{aligned}
 i_R &= g(v_R) = -(|v_R + 1| - |v_R - 1|), \\
 i_r &= g(v_r) = -(|v_r + 1| - |v_r - 1|).
 \end{aligned} \quad (38)$$

The terminal currents and voltages of the memristors A and B satisfy the relation

$$\left. \begin{aligned}
 i_A &= W_A(\varphi_A) v_A = W_A(\varphi_A) (v_2 - v_1), \\
 i_B &= W_B(\varphi_B) v_B = W_B(\varphi_B) (v_1 - v_2),
 \end{aligned} \right\} \quad (39)$$

respectively.

We show the constitutive relations and memductances of the flux-controlled memristors in Figures 14 and 15, respectively. Equation (36) is recast into the form:

$$\left. \begin{aligned}
 &\text{Dynamics of memristor-coupled two-cell CNN} \\
 \frac{dv_1}{dt} &= -v_1 + g(v_1) + W_A(\varphi_A)(v_2 - v_1) + j(t), \\
 \frac{dv_2}{dt} &= -v_2 + g(v_2) + W_B(\varphi_B)(v_1 - v_2), \\
 \frac{d\varphi_A}{dt} &= v_A = v_2 - v_1, \\
 \frac{d\varphi_B}{dt} &= v_B = v_1 - v_2.
 \end{aligned} \right\} \quad (40)$$

Note that the memristor A is active since $W_A(\varphi_A) \leq 0$. On the contrary, the memristor B is passive since $W_B(\varphi_B) \geq 0$. Observe that the memristors switch “off” and “on” at irregular intervals as shown in Figure 16. Furthermore, the two cells are connected when either or both of the memristors switches “on”. We show the trajectory of Eq. (36) and its associated Poincaré map in Figure 17. Observe that Eq. (36) can exhibit a chaotic attractor. Thus, we conclude as follow:

The non-autonomous memristor-coupled two-cell CNN defined by Eq. (36) can exhibit a chaotic attractor. The two flux-controlled memristors in Figure 13 switch “off” and “on” at irregular intervals. Furthermore, the two cells are connected when either or both of the memristors switches “on”.

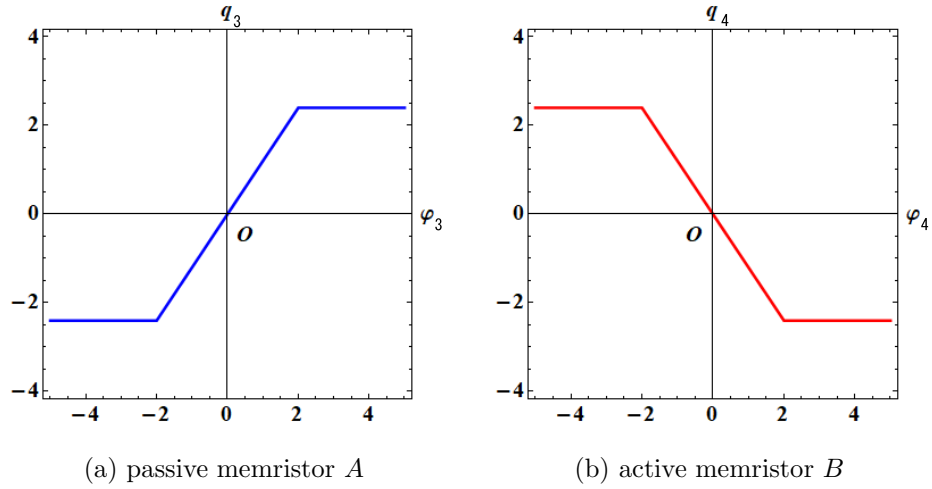


Figure 14: Constitutive relations of the memristor A and the memristor B .

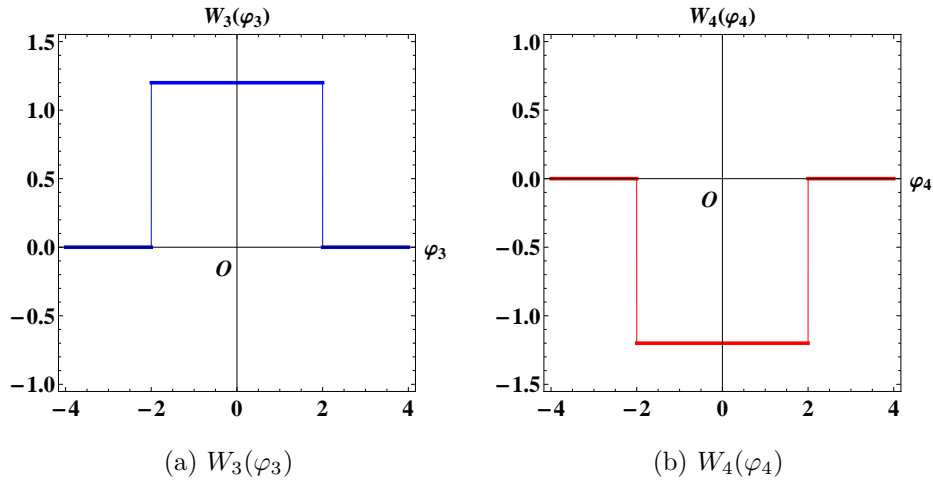


Figure 15: The memductance $W_3(\varphi_3)$ of the passive memristor A and the memductance $W_4(\varphi_4)$ of the active memristor B .

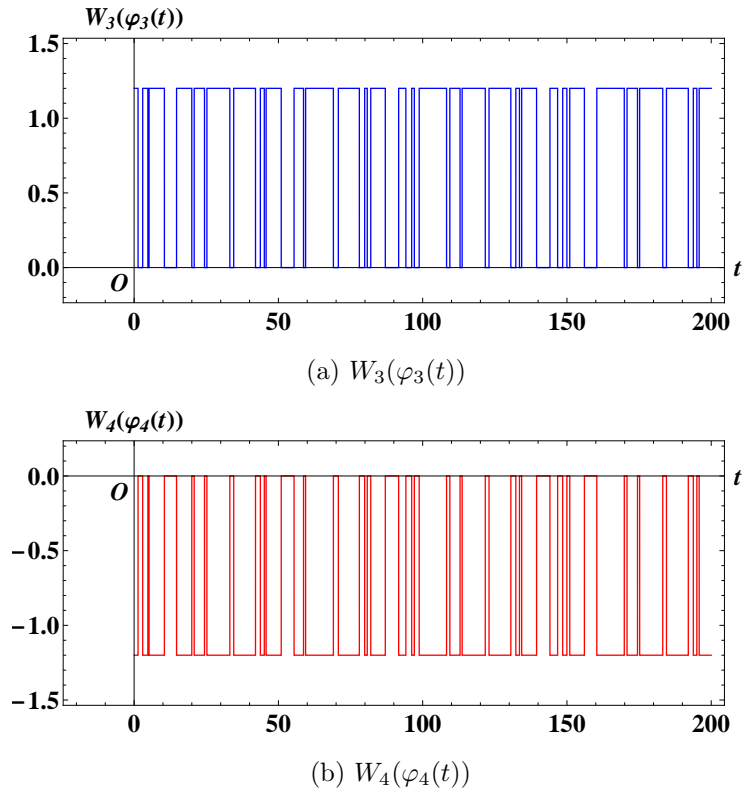


Figure 16: Waveforms of the memductance $W_3(\varphi_3)$ of the passive memristor A (top) and the memductance $W_4(\varphi_4)$ of the active memristor B (bottom). These memristors switch “off” and “on” irregularly.

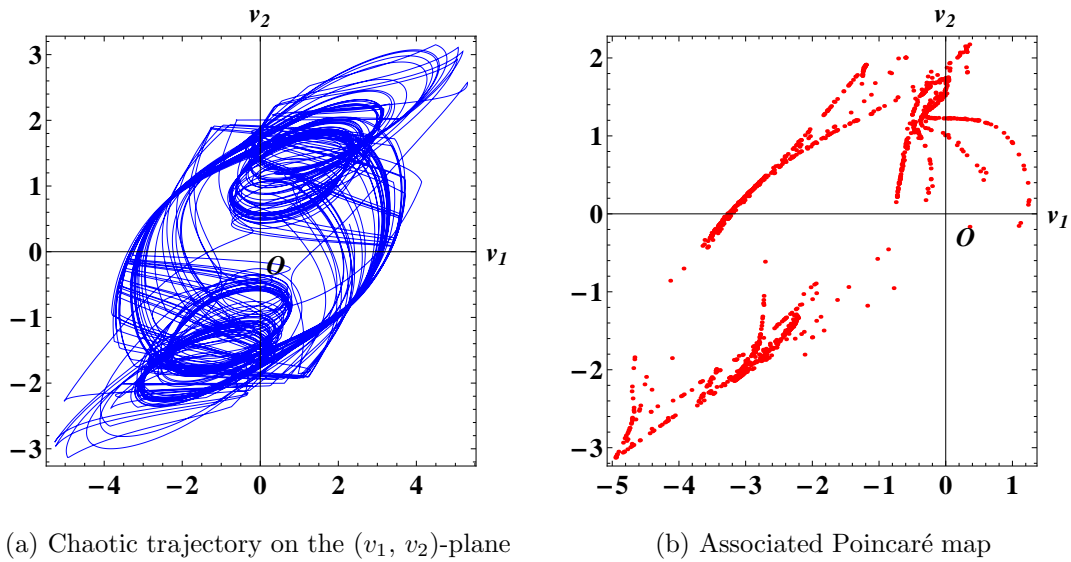


Figure 17: Chaotic trajectory of Eq. (36) and associated Poincaré map. Compare the two attractors in Figures 12 and 17. Initial condition: $v_1(0) = 0, v_2 = 0, \varphi_3(0) = 0, \varphi_4(0) = 0$.

4.4 Similarity between memristors and neurons

In this subsection, we show that there is the similarity between memristors and neurons. The neuron has an “excitatory” synapse and an “inhibitory” synapse. Synapses are junctions that allow a neuron to transmit a signal to another cell. They can either be excitatory or inhibitory. The inhibitory synapses decrease the likelihood of the firing action potential of a cell, while the excitatory synapses increase its likelihood of the firing action potential of a cell.

The memristors in Figure 13 transmit signals from one cell to another cell at irregular intervals. The instantaneous powers of the memristor A and B are given by

$$\begin{aligned} p_A(t) &\triangleq v_A(t) i_A(t) \\ &= W_A(\varphi_A(t)) (v_2(t) - v_1(t))^2 \leq 0, \end{aligned} \quad (41)$$

and

$$\begin{aligned} p_B(t) &\triangleq v_B(t) i_B(t) \\ &= W_B(\varphi_B(t)) (v_1(t) - v_2(t))^2 \geq 0, \end{aligned} \quad (42)$$

respectively, where $W_A(\varphi_A) \leq 0$ and $W_B(\varphi_B) \geq 0$.

It follows that the instantaneous power $p_B(t)$ flows into the cell 2. Similarly, the instantaneous power $p_A(t)$ flows into the cell 1 with the current source $j(t)$, that is, $-p_A(t)$ flows out of it, since $p_A(t)$ is negative.³ Thus, the memristor B corresponds to the “excitatory synapse”, and the memristor A corresponds to the “inhibitory synapse”. The chaotic oscillation of Eq. (36) depends on a delicate balance between the powers $p_A(t)$ and $p_B(t)$.

5 Modified CNN

Consider the modified CNN shown in Figure 18. In this system, the output y_{ij} and the state v_{ij} of each cell is related via the sign function⁴

$$y_{ij} = \text{sgn}(v_{ij}) \triangleq \begin{cases} 1 & v_{ij} > 0, \\ 0 & v_{ij} = 0, \\ -1 & v_{ij} < 0. \end{cases} \quad (43)$$

The switch S is used to disconnect all signals, namely, the output y_{kl} , the input u_{kl} , the threshold z , and the state v_{ij} .

Let us calculate the voltage v_R across the resistor R , which is connected to the switch S . It is given by

$$\begin{aligned} v_R &= \left(\sum_{k, l \in N_{ij}, k \neq i, l \neq j} a_{kl} y_{kl} + \sum_{k, l \in N_{ij}} b_{kl} u_{kl} + z + v_{ij} \right) - v_{ij} \\ &= \left(\sum_{k, l \in N_{ij}, k \neq i, l \neq j} a_{kl} y_{kl} + \sum_{k, l \in N_{ij}} b_{kl} u_{kl} + z \right). \end{aligned} \quad (44)$$

³Note the direction of the power flow and the buffer in Figure 13 provides an input-output isolation.

⁴The sign function can be approximated by using the saturation non-linearity of the Op amp, and by normalizing its output voltage.

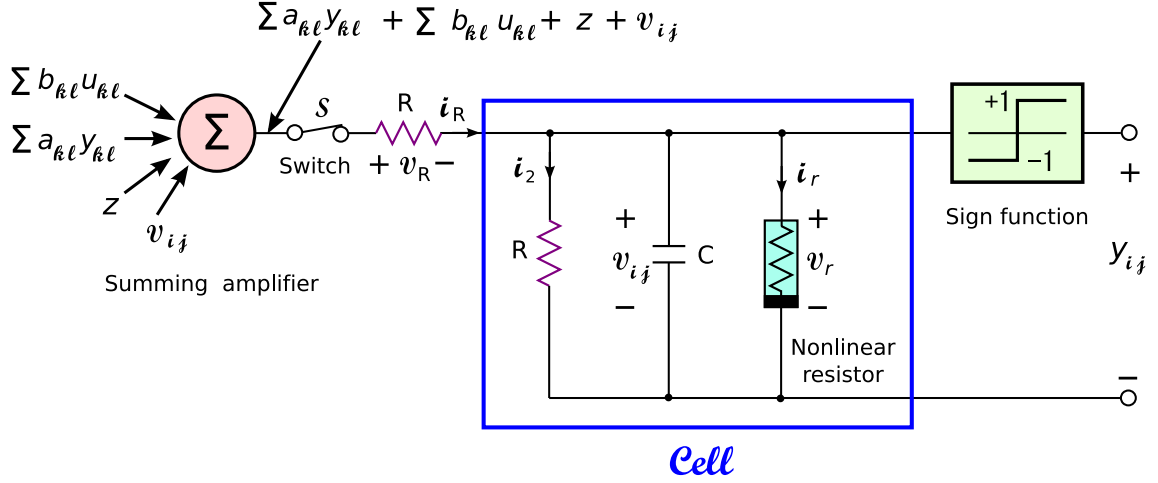


Figure 18: Modified CNN circuit. The switch S is used to disconnect the cell from the summing amplifier (pink).

(1) Parameters: $R = 1$, $C = 1$.

(2) The $v - i$ characteristic of the nonlinear resistor (light blue) is given by $i_r = f_r(v_r) \triangleq -0.5 a (|v_r + 1| - |v_r - 1|)$, where a is a constant.

(3) The output voltage of the summing amplifier is given by
$$\sum_{k, l \in N_{ij}, k \neq i, l \neq j} a_{kl} \operatorname{sgn}(v_{kl}) + \sum_{k, l \in N_{ij}} b_{kl} u_{kl} + z + v_{ij}.$$

(4) The above output voltage contains the voltage v_{ij} of the capacitor C (the last term).

(5) The above sum
$$\sum_{k, l \in N_{ij}, k \neq i, l \neq j} a_{kl} \operatorname{sgn}(v_{kl})$$
 does not contain the term $a_{ij} \operatorname{sgn}(v_{ij})$ ($k = i$, $l = j$).

(6) The output y_{ij} and the state v_{ij} of each cell are related via the sign function (green): $y_{ij} = \operatorname{sgn}(v_{ij})$.

(7) The two linear resistors (purple) have the same resistance R . Thus, we used the same symbol R and color.

Thus, the dynamics of the modified CNN is given by

$$\begin{aligned} C \frac{dv_{ij}}{dt} &= -\frac{v_{ij}}{R} - i_r + \frac{v_R}{R} \\ &= -\frac{v_{ij}}{R} - f_r(v_r) + \frac{\left(\sum_{k, l \in N_{ij}, k \neq i, l \neq j} a_{kl} y_{kl} + \sum_{k, l \in N_{ij}} b_{kl} u_{kl} + z \right)}{R}, \end{aligned} \quad (45)$$

$(i, j) \in \{1, \dots, M\} \times \{1, \dots, N\},$

where

(a) $C = R = 1$.

(b) v_{ij} denotes the voltage across the capacitor C .

(c) The symbols y_{kl} and u_{kl} denote the output and input of cell C_{ij} , respectively.

(d) The symbol N_{ij} denotes the r -neighborhood of cell C_{ij} .

(e) The symbols a_{kl} , b_{kl} , and z denote the feedback, control, and threshold template parameters, respectively. The matrices $A = [a_{kl}]$ and $B = [b_{kl}]$ are referred to as the feedback template A and the feed-forward (input) template B , respectively.

(f) The characteristic of the nonlinear resistor is given by

$$i_r = f_r(v_r) = -0.5 a (|v_r + 1| - |v_r - 1|), \quad (46)$$

where a is a constant.⁵

Substituting Eq. (46) into Eq.(45), and using the relations $C = R = 1$, $v_r = v_{ij}$, $a_{0,0} = a$, we obtain

Dynamics of the modified CNN

$$\begin{aligned} \frac{dv_{ij}}{dt} &= -v_{ij} + 0.5 a_{0,0} (|v_{ij} + 1| - |v_{ij} - 1|) \\ &+ \sum_{k, l \in N_{ij}, k \neq i, l \neq j} a_{kl} \operatorname{sgn}(v_{kl}) + \sum_{k, l \in N_{ij}} b_{kl} u_{kl} + z, \end{aligned} \quad (47)$$

$$(i, j) \in \{1, \dots, M\} \times \{1, \dots, N\}.$$

If we restrict the neighborhood radius of every cell to 1, and if we assume that the feedback and control template parameters do not vary with space, then the template $\{A, B, z\}$ is fully specified by 19 parameters, which are the elements of two 3×3 matrices A and B , namely

$$A = \begin{array}{|c|c|c|} \hline a_{-1,-1} & a_{-1,0} & a_{-1,1} \\ \hline a_{0,-1} & a_{0,0} & a_{0,1} \\ \hline a_{1,-1} & a_{1,0} & a_{1,1} \\ \hline \end{array}, \quad B = \begin{array}{|c|c|c|} \hline b_{-1,-1} & b_{-1,0} & b_{-1,1} \\ \hline b_{0,-1} & b_{0,0} & b_{0,1} \\ \hline b_{1,-1} & b_{1,0} & b_{1,1} \\ \hline \end{array}, \quad (48)$$

and a real number $z \in [1, 2]$. As stated in Sec. 2.1, the feedback and control template parameters can be described as follow:

$$a_{kl} \triangleq a_{k-i, l-j}, \quad b_{kl} \triangleq b_{k-i, l-j}. \quad (49)$$

5.1 Template parameter $a_{0,0}$

The following sum in Eq. (47):

$$\sum_{k, l \in N_{ij}, k \neq i, l \neq j} a_{kl} \operatorname{sgn}(v_{kl}), \quad (50)$$

does *not* contain the term:

$$a_{kl} \operatorname{sgn}(v_{kl}) \Big|_{k=i, l=j} = a_{ij} \operatorname{sgn}(v_{ij}). \quad (51)$$

Substituting Eq. (49) into the left-hand side of Eq. (51), we obtain

$$\begin{aligned} a_{kl} \operatorname{sgn}(v_{kl}) \Big|_{k=i, l=j} &= a_{k-i, l-j} \operatorname{sgn}(v_{kl}) \Big|_{k=i, l=j} \\ &= a_{0,0} \operatorname{sgn}(v_{ij}). \end{aligned} \quad (52)$$

Thus, $a_{0,0} \operatorname{sgn}(v_{ij})$ is not included in Eq. (50). That is, the element $a_{0,0}$ of the feedback template A in Eq. (48) is not given. Therefore, we define $a_{0,0}$ by setting $a_{0,0} = a$, where a is the parameter of the nonlinear resistor, which is given by Eq. (46).

⁵If we use the standard piecewise-linear nonlinearity defined by Eq. (46), then we can apply almost all templates of the CNN, since the CNN templates are designed for this nonlinearity [1, 2, 3].

Element $a_{0,0}$ of template A

The element $a_{0,0}$ of the feedback template A is defined by

$$a_{0,0} = a, \quad (53)$$

where a is the parameter of the nonlinear resistor defined by

$$i_r = -0.5 a (|v_r + 1| - |v_r - 1|). \quad (54)$$

The other elements a_{kl} of A are defined by the coefficients of the output y_{kl} , that is,

$$a_{kl} y_{kl} = a_{kl} \operatorname{sgn}(v_{kl}). \quad (55)$$

5.2 Gray-scale edge detection

Let us consider the *gray-scale edge detection template* [1, 2]

$$A = \begin{array}{|c|c|c|} \hline 0 & 0 & 0 \\ \hline 0 & 2 & 0 \\ \hline 0 & 0 & 0 \\ \hline \end{array}, \quad B = \begin{array}{|c|c|c|} \hline -1 & -1 & -1 \\ \hline -1 & 8 & -1 \\ \hline -1 & -1 & -1 \\ \hline \end{array}, \quad z = \boxed{-0.5}. \quad (56)$$

The initial condition for v_{ij} is given by

$$v_{ij}(0) = 0, \quad (57)$$

and the input u_{kl} is equal to a given gray scale image. The boundary condition is given by

$$v_{k^*l^*} = 0, \quad u_{k^*l^*} = 0, \quad (58)$$

where k^*l^* denotes boundary cells. This template can extract edge of objects in gray scale image as shown in Figure 19. Observe that the modified CNN (47) can hold a binary output image, even if the switch S in Figure 18 is turned off at $t = 80$. That is, the output binary state can not be changed by switching off.

5.3 Shadow projection

Consider the *shadow projection template* [1, 2]

$$A = \begin{array}{|c|c|c|} \hline 0 & 0 & 0 \\ \hline 0 & 2 & 2 \\ \hline 0 & 0 & 0 \\ \hline \end{array}, \quad B = \begin{array}{|c|c|c|} \hline 0 & 0 & 0 \\ \hline 0 & 2 & 0 \\ \hline 0 & 0 & 0 \\ \hline \end{array}, \quad z = \boxed{0}. \quad (59)$$

The initial condition for v_{ij} is given by

$$v_{ij}(0) = 1, \quad (60)$$

and the input u_{kl} is equal to a given binary image. The boundary condition is given by

$$v_{k^*l^*} = 0, \quad u_{k^*l^*} = 0, \quad (61)$$

where k^*l^* denotes boundary cells. This template can project onto the left shadow of all objects illuminated from the right as shown in Figure 20. Observe that the modified CNN (47) can hold a binary output image, even if the switch S is turned off at $t = 40$. That is, the output binary state can not be changed by switching off S as stated above.

5.4 Behavior of the isolated cell after switch-off

Assume that the switch S in Figure 18 is turned off at $t = t_0$. Then, the dynamics of the cell is given by

$$\frac{dv_{ij}}{dt} = -v_{ij} + 0.5 a_{0,0} (|v_{ij} + 1| - |v_{ij} - 1|), \quad (62)$$

$$(i, j) \in \{1, \dots, M\} \times \{1, \dots, N\}.$$

Let us study the behavior of Eq. (62) for the three cases: $a_{0,0} > 1$, $a_{0,0} = 1$, and $a_{0,0} \leq 1$.

1. **Case 1.** $a_{0,0} > 1$.

The driving-point plot of Eq. (62) for $a_{0,0} = 2$ is shown in Figure 10. From Eq. (28), we obtain

$$\left. \begin{array}{l} \text{if } v_{ij}(t_0) < 0, \quad \text{then } \lim_{t \rightarrow \infty} v_{ij}(t) \rightarrow -2, \\ \text{if } v_{ij}(t_0) > 0, \quad \text{then } \lim_{t \rightarrow \infty} v_{ij}(t) \rightarrow 2, \\ \text{if } v_{ij}(t_0) = 0, \quad \text{then } v_{ij}(t) = 0, \end{array} \right\} \quad (63)$$

where $t > t_0$. Since the solution $v_{ij}(t)$ can not move across the origin, the output $y_{ij}(t)$ satisfies the following relations:

$$\left. \begin{array}{l} (1) \quad \text{if } y_{ij}(t_0) = \text{sgn}(v_{ij}(t_0)) = -1, \\ \quad \quad \text{then } y_{ij}(t) = \text{sgn}(v_{ij}(t)) = -1. \\ (2) \quad \text{if } y_{ij}(t_0) = \text{sgn}(v_{ij}(t_0)) = 1, \\ \quad \quad \text{then } y_{ij}(t) = \text{sgn}(v_{ij}(t)) = 1. \\ (3) \quad \text{if } y_{ij}(t_0) = \text{sgn}(v_{ij}(t_0)) = 0, \\ \quad \quad \text{then } y_{ij}(t) = \text{sgn}(v_{ij}(t)) = 0, \end{array} \right\} \quad (64)$$

where $t > t_0$. Thus, the output binary state can not be changed even if we turn off the switch S at $t = t_0$.

2. **Case 2.** $a_{0,0} < 1$.

We show the driving-point plot of Eq. (62) for $a_{0,0} = -1$ in Figure 21. Observe that the origin is a stable equilibrium point. Thus, any trajectory tends to the origin, that is, $v_{ij}(t) \rightarrow 0$ as $t \rightarrow \infty$. Since the solution $v_{ij}(t)$ for $t > t_0$ can not move across the origin, Eq. (64) also holds. That is, the output $y_{ij}(t) = \text{sgn}(v_{ij}(t))$ does not change (except for $t = \infty$), even if we turn off the switch S at $t = t_0$.

3. **Case 3.** $a_{0,0} = 1$.

We show the driving-point plot of Eq. (62) for $a_{0,0} = 1$ in Figure 22. Observe that Eq. (62) has an invariant set D . Any trajectories outside of D tends to the boundary of this set. Furthermore, the solution $v_{ij}(t)$ for $t > t_0$ can not move across D . Thus, Eq. (64) also holds, that is, the output binary state can not be changed even if we turn off the switch S at $t = t_0$.

We conclude that the modified CNN (47) can hold a binary output image even if all cells are disconnected from the summing amplifier and no signal is supplied to the cell. However, we should assume that $a_{0,0} > 1$. It is due to the reason that if $a_{0,0} < 1$, then the physical circuit, for example, the sign function circuit, may not work properly in the presence of noise when $|v_{ij}(t)|$ becomes sufficiently small. Furthermore, if $a_{0,0} = 0$, then the qualitative behavior of Eq. (62) is greatly changed by the small perturbation of $a_{0,0}$.

Note that the modified CNN requires power to maintain the output image, since the isolated cell has a nonlinear active resistor. That is, the output image is lost immediately (*volatile*) when the power is interrupted. From our computer simulations⁶, we obtain the following result:

⁶If the input image size is 256×256 , we have to solve a system of 65536 first-order differential equations. Thus, we used the simple Euler method for solving Eq. (47). It is the most basic method for numerical integration.

Assume $a_{00} > 1$. Then the modified CNN (47) can hold a binary output image even if all cells are disconnected from the summing amplifier and no signal is supplied to the cell after a certain point of time. The modified CNN requires power to maintain the output image, that is, it is *volatile*.

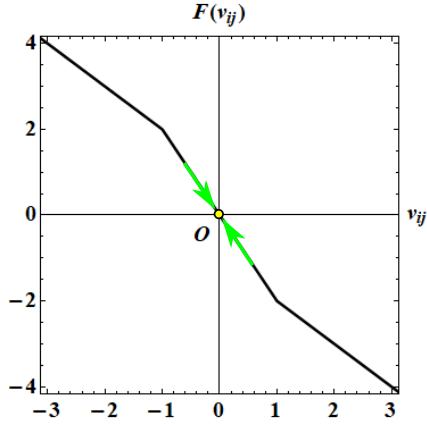


Figure 21: Driving-point plot of Eq. (62) with $a_{0,0} = -1$. Any trajectory tends to the origin, that is, the origin is a stable equilibrium point.

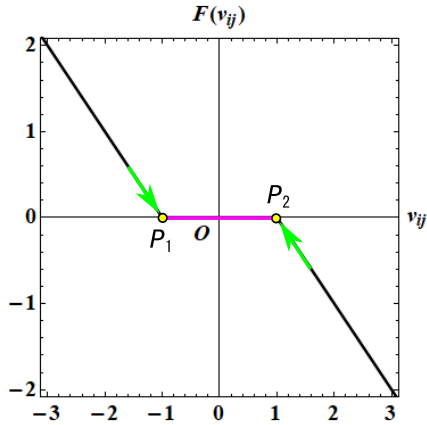


Figure 22: Driving-point plot of Eq. (62) with $a_{0,0} = 1$. The region $D \triangleq [P_1 \leq v_{ij} \leq P_2]$ is an invariant set. That is, any trajectory starting inside D cannot escape from it. Any trajectories outside of D tends to the boundary of this set, that is, P_1 or P_2 .

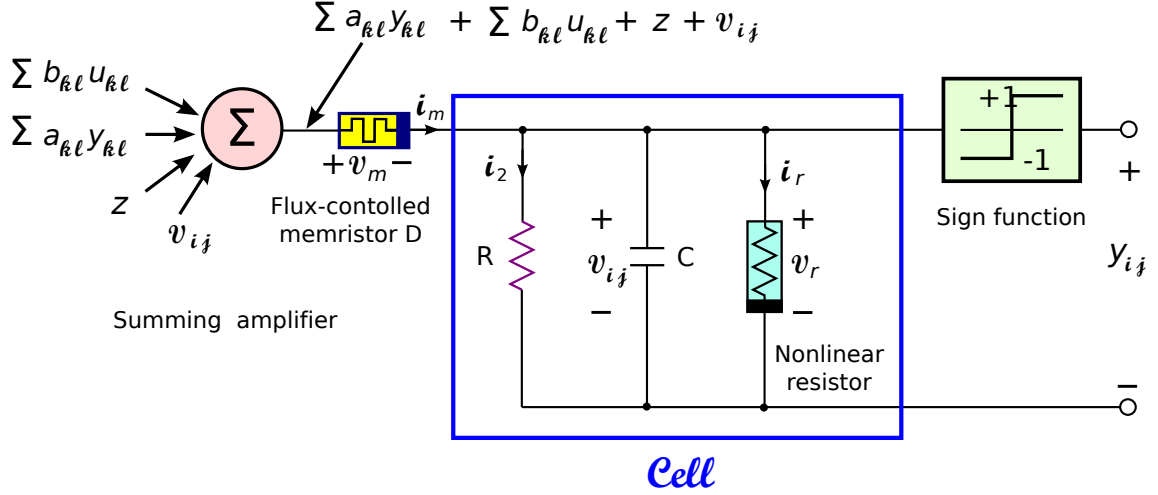


Figure 23: Memristor CNN circuit.

(1) Parameters: $R = 1$, $C = 1$.

(2) The $v - i$ characteristic of the nonlinear resistor (light blue) is given by $i_r = f_r(v_r) \triangleq -0.5 a (|v_r + 1| - |v_r - 1|)$, where a is a constant.

(3) The terminal currents and voltages of the flux-controlled memristor D (yellow) satisfies $i_m = W(\varphi_m) v_m$, where $W(\varphi_m) = 1$ for $-1 < \varphi_m < 1$, and $W(\varphi_m) = 0$ for $\varphi_m \leq -1$ and $\varphi_m \geq 1$.

(4) The output voltage of the summing amplifier (pink) is given by $\sum_{k, l \in N_{ij}, k \neq i, l \neq j} a_{kl} \text{sgn}(v_{kl}) +$

$$\sum_{k, l \in N_{ij}} b_{kl} u_{kl} + z + v_{ij}.$$

(5) The above output voltage contains the voltage v_{ij} of the capacitor C (the last term).

(6) The above sum $\sum_{k, l \in N_{ij}, k \neq i, l \neq j} a_{kl} \text{sgn}(v_{kl})$ does *not* contain the term $a_{ij} \text{sgn}(v_{ij})$ ($k = i$, $l = j$).

(7) The output y_{ij} and the state v_{ij} of each cell are related via the sign function (green): $y_{ij} = \text{sgn}(v_{ij})$.

6 Memoristor CNN

The memristor can switch “off” and “on”, depending on the value of the flux. In this section, we realize the switch S in Figure 18 by using memristors.

Consider the circuit shown in Figure 23. The dynamics of this circuit is given by

$$C \frac{dv_{ij}}{dt} = -\frac{v_{ij}}{R} - i_r + i_m, \quad (65)$$

$$(i, j) \in \{1, \dots, M\} \times \{1, \dots, N\},$$

where $C = R = 1$, and the symbols v_{ij} , i_r , and i_m denote the voltage across the capacitor C , the current through the nonlinear resistor, and the current through the memristor, respectively. Furthermore, this circuit satisfies the following relations:

(a) The output y_{ij} and the state v_{ij} of each cell is related via the sign function

$$y_{ij} = \text{sgn}(v_{ij}). \quad (66)$$

(b) The characteristic of the nonlinear resistor is given by

$$i_r = f_r(v_r) = -0.5 a (|v_r + 1| - |v_r - 1|), \quad (67)$$

where a is a constant.

(c) The terminal voltage v_m and the terminal current i_m of the memristor is given by

$$i_m = W(\varphi_m)v_m, \quad (68)$$

where the flux φ_m of the memristor is defined by

$$\varphi_m = \int_{-\infty}^t v_m dt. \quad (69)$$

(d) The voltage v_m across the memristor is given by

$$v_m = \left(\sum_{k, l \in N_{ij}, k \neq i, l \neq j} a_{kl} y_{kl} + \sum_{k, l \in N_{ij}} b_{kl} u_{kl} + z \right). \quad (70)$$

Note that the first term does not contain $a_{ij} \operatorname{sgn}(v_{ij})$, where $k = i$, $l = j$.

(e) Each cell has *only one memristor*.

Substituting Eqs. (67), (68) into Eq. (65), and using the relations $C = R = 1$, $v_r = v_{ij}$, we obtain

Dynamics of the memristor CNN

$$\frac{dv_{ij}}{dt} = -v_{ij} + 0.5 a (|v_{ij} + 1| - |v_{ij} - 1|) + W(\varphi_m)v_m, \quad (71)$$

$$(i, j) \in \{1, \dots, M\} \times \{1, \dots, N\}.$$

As stated in Sec. 2.1, if we restrict the neighborhood radius of every cell to 1, and if we assume that the feedback and control template parameters do not vary with space, then the templates are fully specified by 19 parameters, which are the elements of two 3×3 matrices A and B , namely

$$A = \begin{array}{|c|c|c|} \hline a_{-1,-1} & a_{-1,0} & a_{-1,1} \\ \hline a_{0,-1} & a_{0,0} & a_{0,1} \\ \hline a_{1,-1} & a_{1,0} & a_{1,1} \\ \hline \end{array}, \quad B = \begin{array}{|c|c|c|} \hline b_{-1,-1} & b_{-1,0} & b_{-1,1} \\ \hline b_{0,-1} & b_{0,0} & b_{0,1} \\ \hline b_{1,-1} & b_{1,0} & b_{1,1} \\ \hline \end{array}, \quad (72)$$

and a real number z , where $a_{0,0} = a$ (a is the parameter of the nonlinear resistor defined by Eq. (67)).⁷

6.1 Dilation

Let us consider the *dilation template* [1, 2]

$$A = \begin{array}{|c|c|c|} \hline 0 & 0 & 0 \\ \hline 0 & 2 & 0 \\ \hline 0 & 0 & 0 \\ \hline \end{array}, \quad B = \begin{array}{|c|c|c|} \hline 0 & 1 & 0 \\ \hline 1 & 1 & 1 \\ \hline 0 & 1 & 0 \\ \hline \end{array}, \quad z = \boxed{4.5}. \quad (73)$$

The initial condition for v_{ij} is given by

$$v_{ij}(0) = 0, \quad (74)$$

⁷ The term $a_{ij} \operatorname{sgn}(v_{ij}) = a_{0,0} \operatorname{sgn}(v_{ij})$ is not included in Eq. (70), as shown in Sec. 5. Therefore, we have to define the element $a_{0,0}$ of the template A by setting $a_{0,0} = a$.

and the input u_{kl} is equal to a given binary image. The boundary condition is given by

$$v_{k^*l^*} = -1, \quad u_{k^*l^*} = -1, \quad (75)$$

where k^*l^* denotes boundary cells. This template can be used to grow a layer of pixels around objects.

Assume that the memductance $W(\varphi_m)$ is given by

$$W(\varphi_m) \triangleq \begin{cases} 1 & -1 \leq \varphi_m \leq 1, \\ 0 & \varphi_m < -1, \varphi_m > 1. \end{cases} \quad (76)$$

The constitutive relation and memductance of the memristor is shown in Figure 24. The terminal voltage v_m satisfies

$$\begin{aligned} |v_m| &= \left| \sum_{k,l \in N_{ij}, k \neq i, l \neq j} a_{kl} y_{kl} + \sum_{k,l \in N_{ij}} b_{kl} u_{kl} + z \right| \\ &= \left| \sum_{k,l \in N_{ij}} b_{kl} u_{kl} + 4.5 \right| \\ &= \left| u_{i-1,j} + u_{i,j-1} + u_{i,j} + u_{i,j+1} \right. \\ &\quad \left. + u_{i+1,j} + 4.5 \right| \geq 0.5, \end{aligned} \quad (77)$$

where $u_{kl} = \pm 1$. For example, assume that

$$u_{i-1,j} = u_{i,j-1} = u_{i,j} = u_{i,j+1} = u_{i+1,j} = -1. \quad (78)$$

Then, we obtain

$$\begin{aligned} v_m &= u_{i-1,j} + u_{i,j-1} + u_{i,j} + u_{i,j+1} + u_{i+1,j} + 4.5 \\ &= -5 + 4.5 = -0.5. \end{aligned} \quad (79)$$

From Eq. (69), we obtain

$$\varphi_m(t) = -0.5t, \quad (80)$$

where we assumed $\varphi_m(0) = 0$. Thus,

$$W(\varphi_m(t)) = \begin{cases} 1 & 0 \leq t \leq 2, \\ 0 & t > 2. \end{cases} \quad (81)$$

Hence, the memristor switches “off” for $t > 2$. Our computer simulations are given in Figure 25. Observe that the template (73) can be used to grow a layer of pixels around objects. It can hold a binary output image for $t > 2$, at which all memristors switched “off”. Note that all memristors do *not* switch “off” *synchronously* since their terminal flux are not always identical.

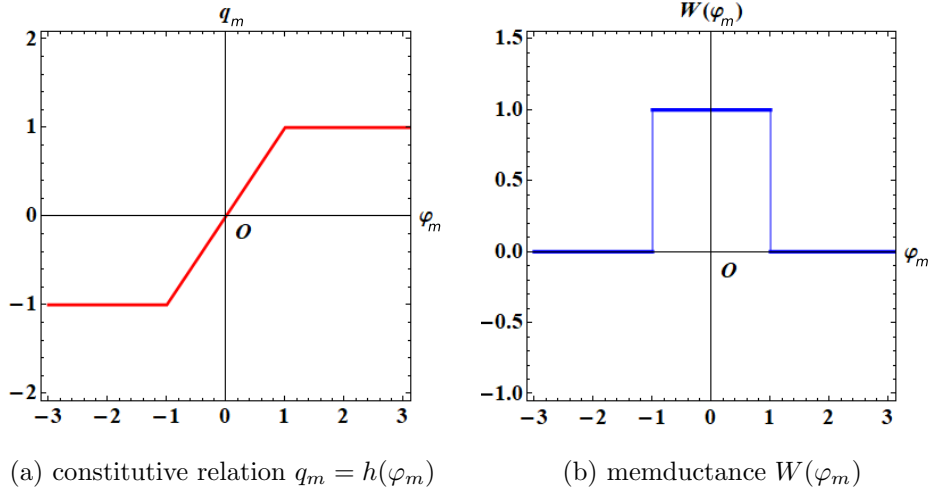


Figure 24: Constitutive relation and memductance of the flux-controlled memristor. The memristor switches “off” and “on” depending on the value of the flux φ_m .

- (a) The constitutive relation of the memristor, which is given by $q_m = h(\varphi_m) \triangleq 0.5(|\varphi_m + 1| - |\varphi_m - 1|)$.
 (b) Memductance $W(\varphi)$ of the memristor, which is defined by $W(\varphi_m) \triangleq \frac{dh(\varphi_m)}{d\varphi_m}$. Thus, $W(\varphi_m) = 1$ for $-1 < \varphi_m < 1$, and $W(\varphi_m) = 0$ for $\varphi_m \leq -1$ and $\varphi_m \geq 1$.

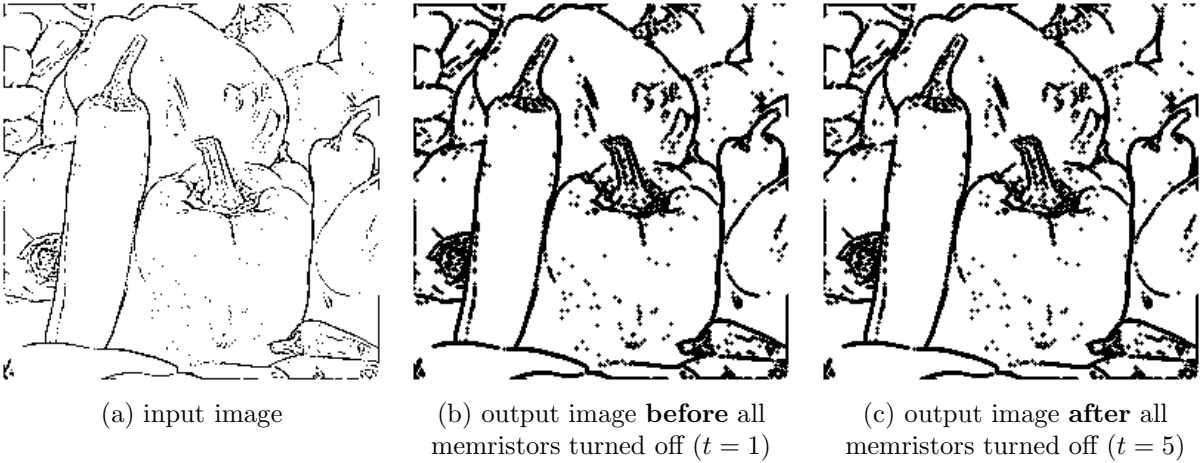


Figure 25: Image-holding property of the memristor CNN (65) with the dilation template (73). This template can be used to grow a layer of pixels around objects. The memristor CNN (65) can hold a binary output image even if all memristors are switched “off”. The memristor in Figure 23 is turned off at $t > 2$. Figures 25(b) and (c) show the output images “before” and “after” all memristors are turned off, respectively. Observe that they are same. The memristor CNN cell size is 256×256 , since the input image size is 256×256 .

6.2 Sharpening with binary output

Let us consider the *sharpening with binary output template*

$$A = \begin{bmatrix} 0 & 0 & 0 \\ 0 & 2 & 0 \\ 0 & 0 & 0 \end{bmatrix}, \quad B = \begin{bmatrix} 0 & -1 & 0 \\ -1 & 5 & -1 \\ 0 & -1 & 0 \end{bmatrix}, \quad (82)$$

$$z = \boxed{0.5}.$$

The initial condition for v_{ij} is given by

$$v_{ij}(0) = 0, \quad (83)$$

and the input u_{kl} is equal to a given *gray-scale* image. The boundary condition is given by

$$v_{k^*l^*} = 0, \quad u_{k^*l^*} = 0, \quad (84)$$

where k^*l^* denotes boundary cells. This template can be used to make an image appear sharper by enhancing edges and convert into a binary image.

Assume that the memductance $W(\varphi_m)$ is given by Eq. (76). The constitutive relation and memductance of the memristor is shown in Figure 24. The terminal voltage v_m satisfies

$$\begin{aligned} |v_m| &= \left| \sum_{k,l \in N_{ij}, k \neq i, l \neq j} a_{kl} y_{kl} + \sum_{k,l \in N_{ij}} b_{kl} u_{kl} + z \right| \\ &= \left| \sum_{k,l \in N_{ij}} b_{kl} u_{kl} - 0.5 \right| \\ &= \left| -u_{i-1,j-1} - u_{i-1,j} - u_{i-1,j+1} \right. \\ &\quad \left. - u_{i,j-1} + 9u_{i,j} - u_{i,j+1} \right. \\ &\quad \left. - u_{i+1,j-1} - u_{i+1,j} - u_{i+1,j+1} - 0.5 \right| \geq 0, \end{aligned} \quad (85)$$

where $-1 \leq u_{kl} \leq 1$ (gray-scale image). Thus, if $v_m(t)$ becomes zero at $t = t_0$, then $\varphi_m(t)$ and $W(\varphi_m(t))$ does not change until $v_m(t) \neq 0$ for $t > t_0$. In this case, all memristor may not switch “off”.

We show our computer simulations in Figure 26. Observe that the template (82) can make the image sharper by enhancing edges and convert into a binary image. Thus, the memoristor CNN (65) can hold a binary output image, even if almost memristos switched “off” as shown in Figure 26(c). Thus, we conclude as follow:

Assume $a_{00} > 1$. Then the memristor CNN in Figure 23 can hold a binary output image, even if almost all memristors switch off.

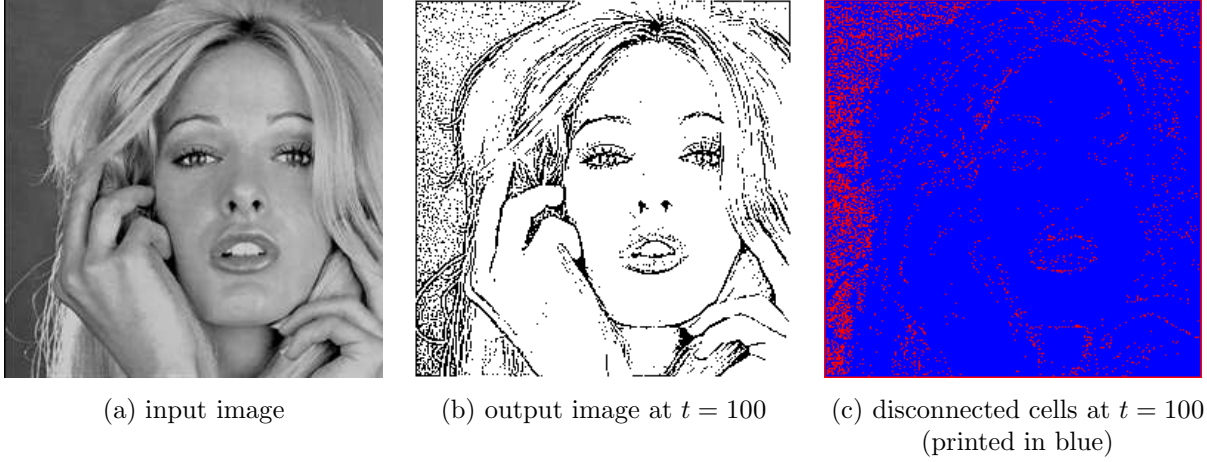


Figure 26: Image-holding property of the memristor CNN (65) with the sharpening with binary output (82). This template can be used to make an image appear sharper by enhancing edges and convert into a binary image, as shown in Figure 26(b). The memristor CNN (65) can hold a binary output image, even if almost memristos switched “off” (printed in blue) as shwon in Figure 26(c). Here, the red point indicates the cell whose memristor still switches “on”. The blue point indicates the cell whose memristor switched “off”, that is, the cell is disconnected from the summing amplifier in Figure 23. The memristor CNN cell size is 256×256 , since the input image size is 256×256 .

7 Effect of a Parasitic Conductance

Consider the case where the memristor in Figure 23 has a parallel parasitic conductance G as shown in Figure 27. Then, the dynamics of the circuit in Figure 23 is modified into

$$C \frac{dv_{ij}}{dt} = -\frac{v_{ij}}{R} - i_r - i_m - i_G, \quad (86)$$

$$(i, j) \in \{1, \dots, M\} \times \{1, \dots, N\},$$

where $C = R = 1$, and the symbols v_{ij} , i_m , i_r , and i_G denote the voltage across the capacitor C , the current through the memristor, and the current trough the nonlinear resistor, and the current through the parallel parasitic conductance G , respectively.

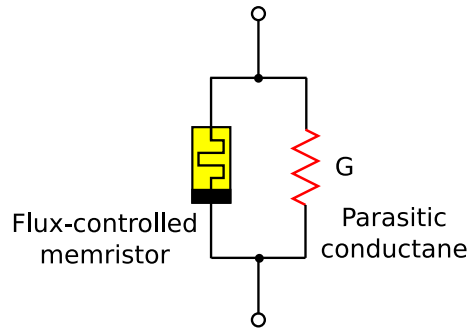


Figure 27: Parasitic conductance G ($0 < G \ll 1$) of the flux-ctrlled memristor.

Furthermore, this circuit satisfies the following relations:

(a) The output y_{ij} and the state v_{ij} of each cell is related via the sign function

$$y_{ij} = \text{sgn}(v_{ij}). \quad (87)$$

(b) The voltage v_m across the memristor is given by

$$v_m = \sum_{k, l \in N_{ij}, k \neq i, l \neq j} a_{kl} y_{kl} + \sum_{k, l \in N_{ij}} b_{kl} u_{kl} + z, \quad (88)$$

where the first sum does not contain $a_{ij} \text{sgn}(v_{ij})$, where $k = i$, $l = j$. The current i_m through the memristor is given by

$$\begin{aligned} i_m &= W(\varphi_m) v_m \\ &= W(\varphi_m) \left(\sum_{k, l \in N_{ij}, k \neq i, l \neq j} a_{kl} y_{kl} + \sum_{k, l \in N_{ij}} b_{kl} u_{kl} + z \right). \end{aligned} \quad (89)$$

where $W(\varphi_m)$ denotes the memductance of the memristor and the flux φ_m of the memristor is defined by

$$\varphi_m = \int_{-\infty}^t v_m dt. \quad (90)$$

(c) The current i_G through the conductance G is given by

$$i_G = G v_m, \quad (91)$$

where $0 < G \ll 1$.

(d) The characteristic of the nonlinear resistor is given by

$$i_r = f_r(v_r) = -0.5 a (|v_r + 1| - |v_r - 1|), \quad (92)$$

where a is a constant.

Substituting Eqs. (89), (91), and (92) into Eq. (86), we obtain

$$\begin{aligned} \frac{dv_{ij}}{dt} &= -v_{ij} + 0.5 a (|v_{ij} + 1| - |v_{ij} - 1|) \\ &\quad + (W(\varphi_m) + G) v_m. \end{aligned} \quad (93)$$

Let us assume that the memductance $W(\varphi_m)$ is given by Eq. (76), that is,

$$W(\varphi_m) \triangleq \begin{cases} 1 & -1 \leq \varphi_m \leq 1, \\ 0 & \varphi_m < -1, \varphi_m > 1. \end{cases} \quad (94)$$

Then the dynamics of Eq. (93) can be described as follow:

1. **Case 1.** $W(\varphi_m) = 1$.
From Eq. (93), we obtain

$$\frac{dv_{ij}}{dt} = -v_{ij} + 0.5 a (|v_{ij} + 1| - |v_{ij} - 1|) + (1 + \epsilon) v_m, \quad (95)$$

where $0 < \epsilon \triangleq G \ll 1$. Substituting Eq. (70) into Eq. (95), we obtain

$$\begin{aligned} \frac{dv_{ij}}{dt} &= -v_{ij} + 0.5 a (|v_{ij} + 1| - |v_{ij} - 1|) \\ &+ (1 + \epsilon) \left(\sum_{k, l \in N_{ij}, k \neq i, l \neq j} a_{kl} y_{kl} + \sum_{k, l \in N_{ij}} b_{kl} u_{kl} + z \right). \end{aligned} \quad (96)$$

Assume that the qualitative behavior of the modified CNN (47) is not affected by the small perturbation of the template $\{A, B, z\}$. Then the output of Eq. (96) is identical to that of the modified CNN, which is given by

$$\begin{aligned} \frac{dv_{ij}}{dt} &= -v_{ij} + 0.5 a (|v_{ij} + 1| - |v_{ij} - 1|) \\ &+ \left(\sum_{k, l \in N_{ij}, k \neq i, l \neq j} a_{kl} y_{kl} + \sum_{k, l \in N_{ij}} b_{kl} u_{kl} + z \right). \end{aligned} \quad (97)$$

2. Case 2. $W(\varphi_m) = 0$.

From Eq. (93), we obtain

$$\frac{dv_{ij}}{dt} = -v_{ij} + 0.5 a (|v_{ij} + 1| - |v_{ij} - 1|) + \epsilon v_m, \quad (98)$$

where $0 < \epsilon \ll 1$. Let us choose the parameter a so that the qualitative behavior of the isolated cell is not affected by the small perturbation ϵv_m . For example, choose $a > 1$. Then, the qualitative behavior of the driving-point plot of Eqs. (95) and (98) is not changed, since ϵv_m and $(1 + \epsilon)v_m$ have the same sign. Thus, the output $y_{ij}(t) = \text{sgn}(v_{ij}(t))$ is not changed by this small perturbation ϵv_m . In this case, Eq. (98) is approximated by

$$\frac{dv_{ij}}{dt} = -v_{ij} + 0.5 a (|v_{ij} + 1| - |v_{ij} - 1|). \quad (99)$$

It follows that there is not much of a difference between the output images of Eqs. (65) and (86). Note that the CNN template $\{A, B, z\}$ is usually designed such that the qualitative behavior is not affected by the small perturbation. In fact, we could not find any difference between the output images of Eqs. (65) and (86) when the template is given by Eq. (73) or Eq. (82). Thus, we conclude as follow:

Assume that the memductance $W(\varphi_m)$ is given by Eq. (76), and assume that the template is given by Eq. (73) or Eq. (82). Then we could not find any difference between the output images of Eqs. (65) and (86).

8 Neuron-like Behavior

The neurons cannot respond to inputs quickly and they cannot generate outputs rapidly, since charging or discharging the membrane potential energy can take time. Furthermore, after firing, the neurons have *refractory period*. In this subsection, we show that the memoristor CNN (65) can exhibit the similar behavior.

8.1 Smoothing with binary output

Let us consider the *smoothing with binary output template* [8]

$$A = \begin{bmatrix} 0 & 1 & 0 \\ 1 & 2 & 1 \\ 0 & 1 & 0 \end{bmatrix}, \quad B = \begin{bmatrix} 0 & 0 & 0 \\ 0 & 0 & 0 \\ 0 & 0 & 0 \end{bmatrix}, \quad z = \boxed{0}. \quad (100)$$

The initial condition for the state v_{ij} is equal to a given gray-scale image. The boundary condition is given by

$$v_{k^*l^*} = 0, u_{k^*l^*} = 0, \quad (101)$$

where k^*l^* denotes boundary cells. This template can be used to smooth (average) a gray-scale image and convert into a binary image. It also deletes the noise from the image as shown in Figure 28.

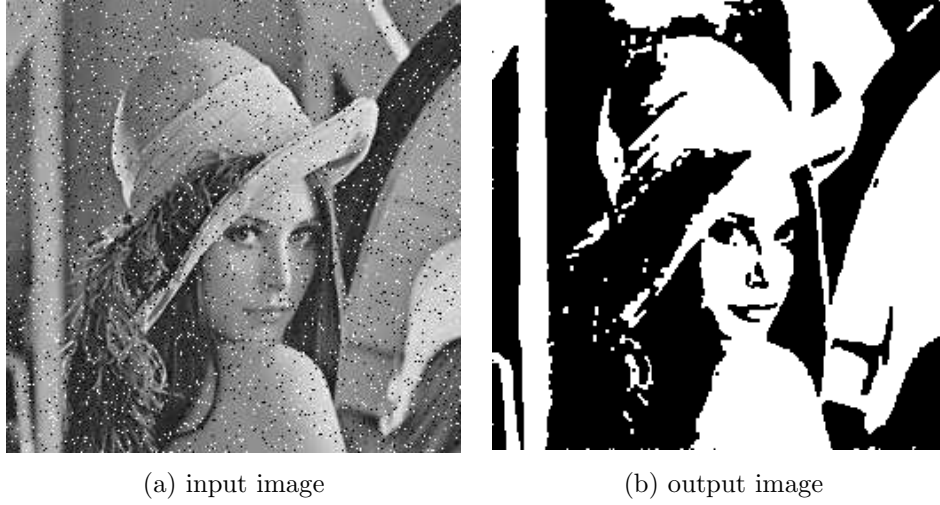


Figure 28: Input and output images for the smoothing with binary output template (100). It can be used to smooth (average) a gray-scale image and convert into a binary image. Hence, it can delete the noise from the image. Image size is 256×256 .

Consider the memristor CNN circuit in Figure 23. Suppose that the flux-controlled memristor has the following constitutive relation and memductance:

$$q_m = h(\varphi_m) \triangleq \begin{cases} 0.5(|\varphi_m - 2| - |\varphi_m - 10|) \\ -0.5(|\varphi_m + 2| - |\varphi_m + 10|), \end{cases} \quad (102)$$

and

$$\begin{aligned} W(\varphi_m) &= \frac{dh(\varphi_m)}{d\varphi_m} \\ &\triangleq \left(\mathfrak{s} \left[|\varphi_m| - 2 \right] - \mathfrak{s} \left[|\varphi_m| - 10 \right] \right) \\ &= \begin{cases} 0 & \varphi_m \leq -10, \\ 1 & -10 < \varphi_m < -2, \\ 0 & -2 \leq \varphi_m \leq 2, \\ 1 & 2 < \varphi_m < 10, \\ 0 & 10 \leq \varphi_m, \end{cases} \end{aligned} \quad (103)$$

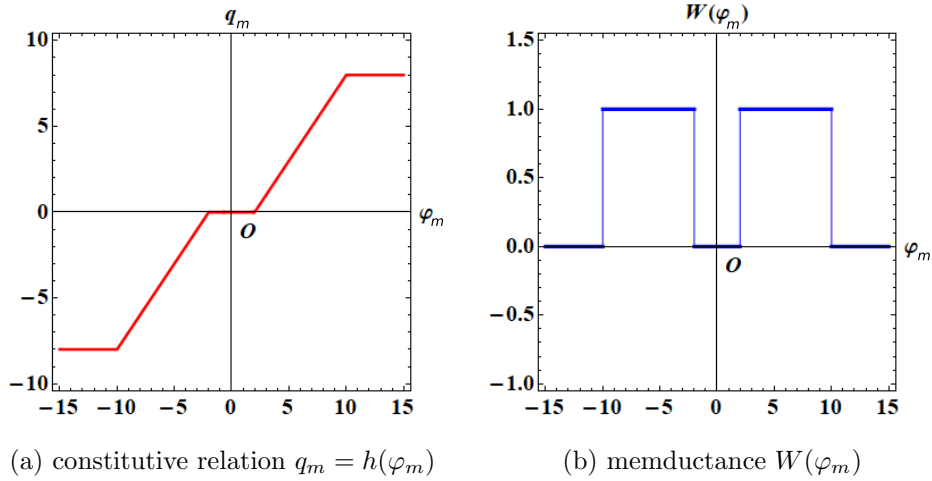


Figure 29: Constitutive relation and memductance of the flux-controlled memristor. The memristor switches off and on depending on the value of the flux φ_m .

(a) The constitutive relation of the memristor, which is defined by $q_m = h(\varphi_m) \triangleq 0.5(|\varphi_m - 2| - |\varphi_m - 10|) - 0.5(|\varphi_m + 2| - |\varphi_m + 10|)$.

(b) Memductance $W(\varphi)$ of the memristor, which is defined by $W(\varphi_m) \triangleq \frac{dh(\varphi_m)}{d\varphi_m} = (\mathfrak{s}[|\varphi_m| - 2] - \mathfrak{s}[|\varphi_m| - 10])$. The symbol $\mathfrak{s}[z]$ denotes the *unit step* function, equal to 0 for $z < 0$ and 1 for $z \geq 0$.

respectively (see Figure 29). Its terminal voltage v_m satisfies

$$\begin{aligned}
v_m(t) &= \sum_{k, l \in N_{ij}, k \neq i, l \neq j} a_{kl} y_{kl}(t) \\
&= a_{-1,0} y_{i-1,j}(t) + a_{0,-1} y_{i,j-1}(t) + a_{0,1} y_{i,j+1}(t) \\
&\quad + a_{1,0} y_{i+1,j}(t) \\
&= y_{i-1,j}(t) + y_{i,j-1}(t) + y_{i,j+1}(t) + y_{i+1,j}(t),
\end{aligned} \tag{104}$$

where

$$\begin{aligned}
a_{-1,0} = a_{0,-1} = a_{0,1} = a_{1,0} &= 1, \\
y_{kl}(t) &\in \{-1, 0, 1\}.
\end{aligned} \tag{105}$$

Thus, the terminal voltage v_m satisfies

$$|v_m(t)| \geq 0. \tag{106}$$

If $v_m(t)$ becomes zero at $t = t_0$, then $W(\varphi_m(t))$ does not change until $v_m(t) \neq 0$ for $t > t_0$. Compare Eq. (106) with Eq. (77).

Our computer simulations are shown in Figures 30 and 31. We explain their results briefly.

1. The memoristor CNN can *not* remove the noise from the input image at the initial stage. It is due to the reason that charging flux to memristors can take time, and the memristor can not switch “on” rapidly.
2. When time t is increased, almost memristors change from the “switch-off” state to the “switch-on” state, and the memoristor CNN (65) can delete the noise from the given image by smoothing. It can also hold the output image even if almost memristors switched “off”.

The detailed behavior of the memoristor CNN (65) can be described as follow:

1. $t = 0.01$

All memristors switched “off”. That is, all cells are printed in blue as shown in Figure 30(b). Thus, the memoristor CNN (65) can only convert the given gray-scale image to the binary image. It cannot delete the noise from the image. It is due to the reason that the memoristor CNN (65) cannot respond to the input quickly, since the memristors cannot switch “on” rapidly.

2. $t = 0.5$, $t = 2$, and $t = 5$

Many memristors change to the “switch-on”, and then they switch “off” again, as shown in Figures 30(c), (d), and (e). Note that all memristors do not change between the “switch-off” and “switch-on” states, *synchronously*. Furthermore, only the cell with a “switched-on memristor” can smooth (average) the given image, and delete the noise.

3. $t = 15$

The memoristor CNN (65) can hold the output image, even if almost all memristors switched “off”. Several cells still switch “on” (they are marked by yellow circles and arrows in Figure 30(f)).

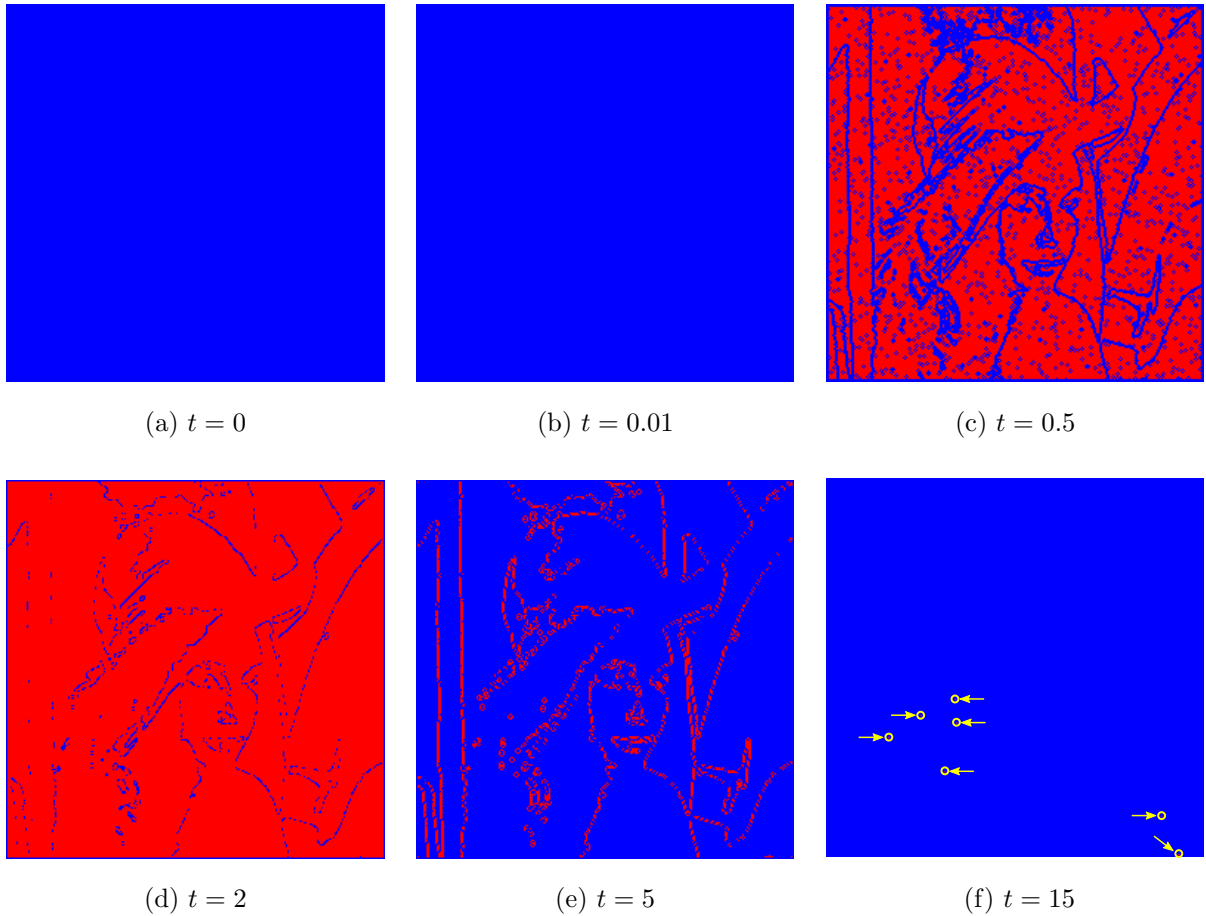


Figure 30: “Switch-on” and “switch-off” states. Red point indicates the cell whose memristor switched “on”, and the blue point indicates the cell whose memristor switched “off”. The memristor CNN cell size is 256×256 , since the input image size is 256×256 .

- (a) All memristors switch “off”. Thus, all cells are printed in blue.
- (b) All memristors switch “off”, since the memristor can not switch “on” rapidly.
- (c) Many memristors is turning from the “switch-off” state (printed in blue) to the “switch-on” state (printed in red).
- (d) Most memristos turn to the “switch-on” (printed in red).
- (e) Most memristos turn from the “switch-on” state (printed in red) to the “switch-off” state (blue), again.
- (f) Almost all memristos are switched “off” (printed in blue), except several cells (marked by yellow circles and arrows).

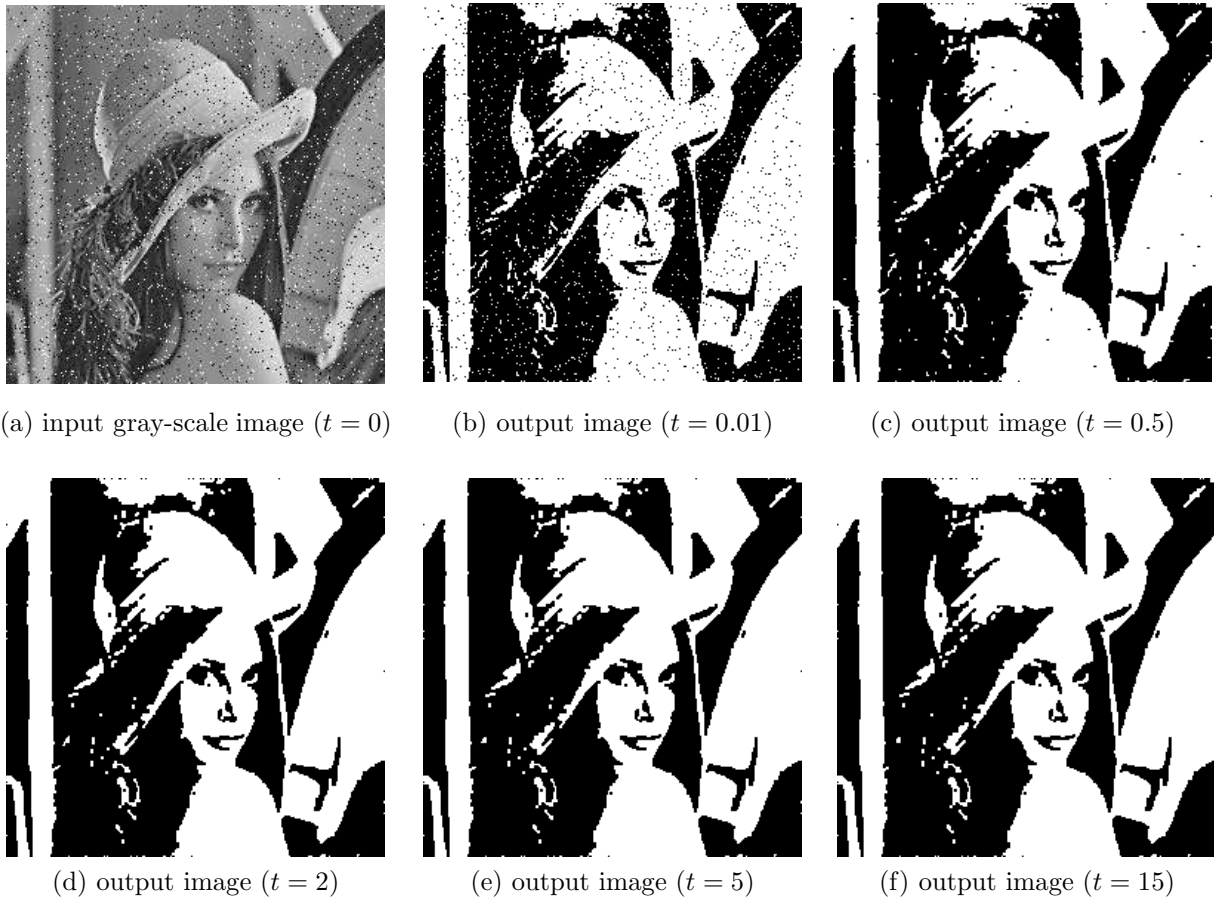


Figure 31: Neuron-like behavior for the memristor CNN (65) with the smoothing with binary output template (100). Observer that the memristor CNN (65) cannot respond to the input quickly, and it can hold the output image even if almost all memristors switch “off”.

(a) Gray-scale input image for the memristor CNN (65). All memristors switch “off”.

(b) The memristor CNN (65) does *not* delete the noise from the image, since **all memristors** still switch “off”, that is, the memristor can not switch “on” rapidly.

(c) The memristor CNN (65) can *not* delete *all noise* from the image, though **many memristors** are turning from the “switch-off” state to the “**switch-on**” state.

(d) The memristor CNN (65) deleted the noise from the image, since **most memristos** turn to the “**switch-on**”.

(e) The memristor CNN (65) deleted the noise from the image. At this point in time, **most memristos** turn from the “switch-on” to the “**switch-off**”, **again**.

(f) The memristor CNN (65) can hold a binary output image, even if **almost all memristos** switched “off”, except for several cells (which is marked by yellow circles and arrows in Figure 30(f)).

8.2 Erosion

Let us consider the *erosion template* [1, 2]

$$A = \begin{bmatrix} 0 & 0 & 0 \\ 0 & 2 & 0 \\ 0 & 0 & 0 \end{bmatrix}, \quad B = \begin{bmatrix} 0 & 1 & 0 \\ 1 & 1 & 1 \\ 0 & 1 & 0 \end{bmatrix}, \quad z = \boxed{-4.5}. \quad (107)$$

The initial condition for v_{ij} is given by

$$v_{ij}(0) = 0, \quad (108)$$

and the input u_{kl} is equal to a given binary image. The boundary condition is given by

$$v_{k^*l^*} = -1, \quad u_{k^*l^*} = -1, \quad (109)$$

where k^*l^* denotes boundary cells. This template can be used to peel off all boundary pixels of binary image objects, as shown in Figure 32.

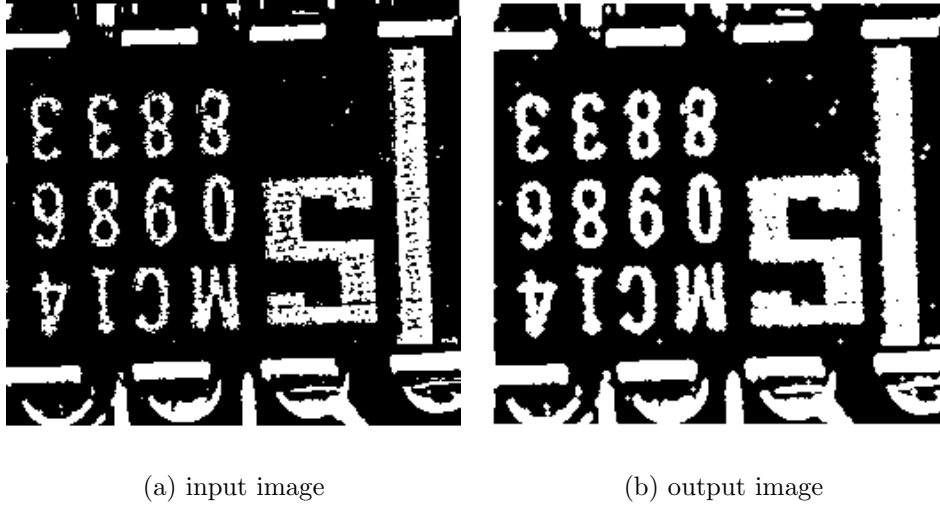


Figure 32: Input and output images for the erosion template (107). It can be used to peel off all boundary pixels of binary image objects. Hence, the text becomes clearly visible by this template. Image size is 256×256 .

Consider the memristor CNN circuit in Figure 23. Suppose that the constitutive relation and memductance of the flux-controlled memristor are given by Eqs. (102) and (103), respectively (see Figure 29). Thus, its terminal voltage v_m satisfies

$$\begin{aligned} |v_m| &= \left| \sum_{k, l \in N_{ij}, k \neq i, l \neq j} a_{kl} y_{kl} + \sum_{k, l \in N_{ij}} b_{kl} u_{kl} + z \right| \\ &= \left| \sum_{k, l \in N_{ij}} b_{kl} u_{kl} + 4.5 \right| \\ &= \left| u_{i-1, j} + u_{i, j-1} + u_{i, j} + u_{i, j+1} \right. \\ &\quad \left. + u_{i+1, j} - 4.5 \right| \geq 0.5, \end{aligned} \quad (110)$$

where

$$\left. \begin{aligned} b_{i-1,j} = b_{i,j-1} = b_{i,j} = b_{i,j+1} = b_{i+1,j} = 1, \\ u_{kl} = \pm 1. \end{aligned} \right\} \quad (111)$$

For example, if we assume that the inputs u_{kl} satisfy

$$u_{i-1,j} = u_{i,j-1} = u_{i,j} = u_{i,j+1} = u_{i+1,j} = 1, \quad (112)$$

then we obtain

$$\begin{aligned} v_m &= u_{i-1,j} + u_{i,j-1} + u_{i,j} + u_{i,j+1} + u_{i+1,j} - 4.5 \\ &= 5 - 4.5 = 0.5. \end{aligned} \quad (113)$$

In this case, we obtain from Eq. (69)

$$\varphi_m(t) = 0.5t, \quad (114)$$

where we assume $\varphi_m(0) = 0$.

Assume next that the constitutive relation and memductance of the flux-controlled memristor are given by Eqs. (102) and (103), respectively. Then, we obtain

$$W(\varphi_m(t)) = \begin{cases} 0 & 0 \leq t < 4, \\ 1 & 4 \leq t \leq 20, \\ 0 & 20 < t, \end{cases} \quad (115)$$

where the input u_{kl} is given by Eq. (112) and $\varphi_m(t) = 0.5t$. Note that other inputs may satisfy the equation $W(\varphi_m(t)) = 1$ more quickly than the above. That is, all memristors do *not* switch “on” *synchronously*, since their terminal flux are not always identical.

Our computer simulations are shown in Figures 33 and 34. The boundary pixels of the given binary image are peeled off, and the text becomes clearly visible. We conclude as follow:

Suppose that the memoristor CNN (65) has the following property:

- a. The feedback, control, and threshold parameters are given by Eq. (100) or (107).
- b. The constitutive relation and the memductance of the flux-controlled memristors are given by Eq. (102) and (103), respectively.

Then, the memoristor CNN (65) can exhibit the following behavior:

1. The memoristor CNN (65) cannot respond to the input quickly, since the memristors cannot switch “on” rapidly.
2. The memoristor CNN (65) can hold the output image even if almost all memristors switch “off” (refractory period).

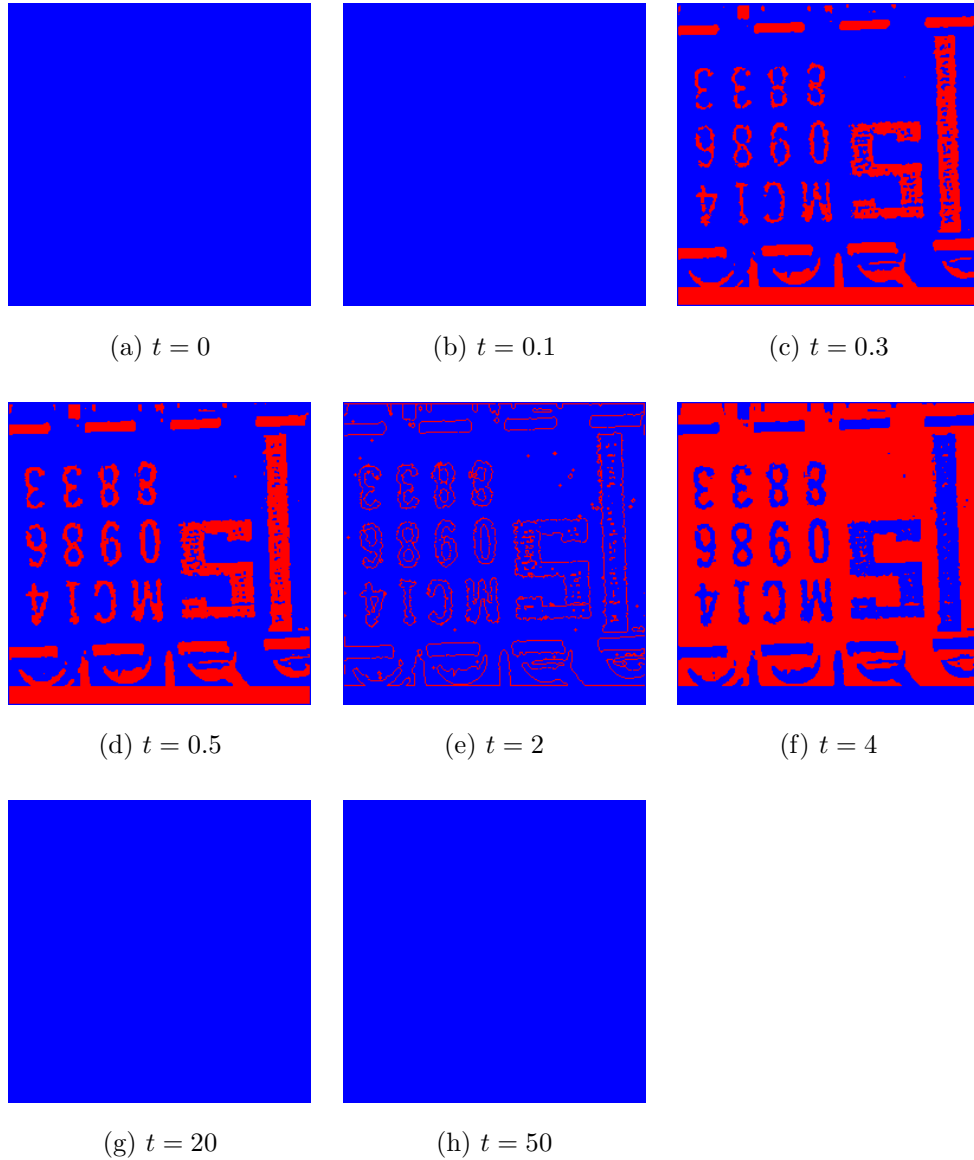


Figure 33: “Switch-on” and “switch-off” states of memristors. Red point indicates the cell whose memristor switched “on”, and the blue point indicates the cell whose memristor switched “off”. The memristor CNN cell size is 256×256 , since the input image size is 256×256 .

(a) All memristors switch “off”. Thus, all cells are printed in blue.

(b) All memristors switch “off”, since the memristor can not switch “on” rapidly.

(c)-(d) Memristors are turning from the “switch-off” state (printed in blue) to the “switch-on” state (printed in red).

(e) “Switch-on” memristors (printed in red) are turning to the “switch-off” (printed in blue).

(f) “Switch-off” memristors (printed in blue), which do *not* have switched “on” *yet*, turn to the “switch-on” state (printed in red).

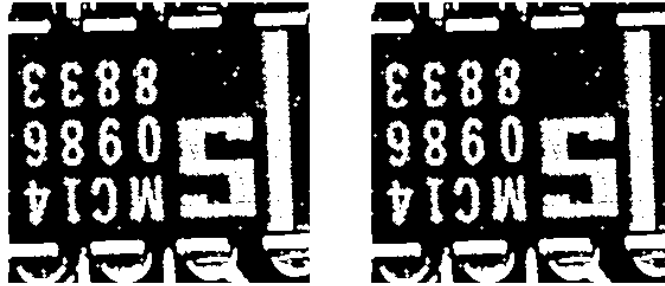
(g)-(h) All memristos switch “off”, again. Thus, all cells are printed in blue.



(a) input binary image ($t = 0$) (b) output image ($t = 0.1$) (c) output image ($t = 0.3$)



(d) output image ($t = 0.5$) (e) output image ($t = 2$) (f) output image ($t = 4$)



(g) output image ($t = 20$) (h) output image ($t = 50$)

Figure 34: Neuron-like behavior for the memoristor CNN (65) with the erosion template (107). Observe that the memoristor CNN (65) cannot respond to the input quickly, and it can hold the output image even if all memristors switch “off”.

(a) Binary input image for the memoristor CNN (65). At this point, all memristors switch “off”. The state $y_{ij} = 0$ is shown in gray.

(b) The memoristor CNN (65) does *not* peel off the boundary pixels, since **all memristors** still switch “off”, that is, the memristor can not switch “on” rapidly.

(c)-(e) The boundary pixels are peeled off gradually, since the memristors are turning to the “switch-on” state from the “switch-off” state.

(f) The color of the cells is changed to “black and white” from “gray and white”.

(g)-(h) The memoristor CNN (65) hold the output image, even if all memristors switch “off”, again (see Figure 33(g) and (h))

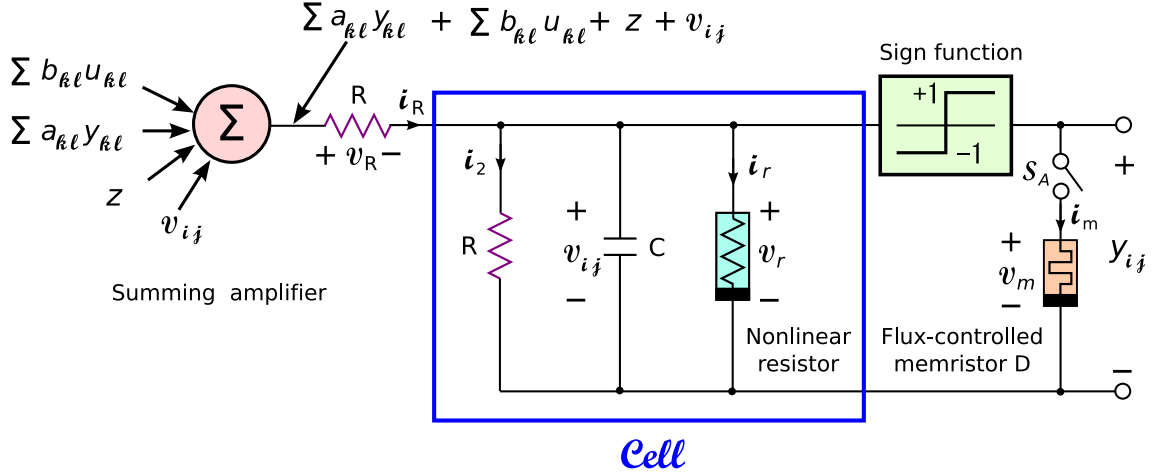


Figure 35: Circuit which can store the time average of the output state y_{ij} . The switch S_A is closed during the time averaging.

(1) Parameters: $R = 1$, $C = 1$.

(2) The $v - i$ characteristic of the nonlinear resistor (light blue) is given by $i_r = f_r(v_r) \triangleq -0.5 a (|v_r + 1| - |v_r - 1|)$, where a is a constant.

(3) The terminal currents and voltages of the flux-controlled memristor D (orange) satisfies $i_m = W(\varphi_m) v_m = \mathfrak{s}[\varphi_m] v_m$. The symbol $\mathfrak{s}[z]$ denotes the *unit step* function, equal to 0 for $z < 0$ and 1 for $z \geq 0$.

(4) The output voltage of the summing amplifier (pink) is given by
$$\sum_{k, l \in N_{ij}, k \neq i, l \neq j} a_{kl} \text{sgn}(v_{kl}) +$$

$$\sum_{k, l \in N_{ij}} b_{kl} u_{kl} + z + v_{ij}.$$

(5) The above output voltage contains the voltage v_{ij} of the capacitor C (the last term).

(6) The above sum
$$\sum_{k, l \in N_{ij}, k \neq i, l \neq j} a_{kl} \text{sgn}(v_{kl})$$
 does *not* contain the term $a_{ij} \text{sgn}(v_{ij})$ ($k = i$, $l = j$).

(7) The output y_{ij} and the state v_{ij} of each cell are related via the sign function (green): $y_{ij} = \text{sgn}(v_{ij})$.

9 Suspend and Resume Feature

The *suspend* and *resume feature* are useful when we want to save the current state, and continue work later from the same state. We show that the memristor CNN has the similar feature.

Let us consider the memristor CNN in Figure 35. The parameters are given by

$$E = 1, J = 0.5, R = 1, C = 1. \quad (116)$$

The characteristic of the nonlinear resistor is given by

$$i_r = f(v_r) = -0.5 a (|v_r + 1| - |v_r - 1|), \quad (117)$$

where a is a constant. The constitutive relation and memductance of the flux-controlled memristor are given by

$$q_m = h(\varphi_m) \triangleq 0.5 (|\varphi_m| + \varphi_m), \quad (118)$$

and

$$W(\varphi_m) = \frac{dh(\varphi_m)}{d\varphi_m} = \mathfrak{s}[\varphi_m], \quad (119)$$

respectively (see Figure 36), where q_m and φ_m denote the charge and the flux of the memristor, respectively, the symbol $\mathfrak{s}[z]$ denotes the *unit step* function, equal to 0 for $z < 0$ and 1 for $z \geq 0$.

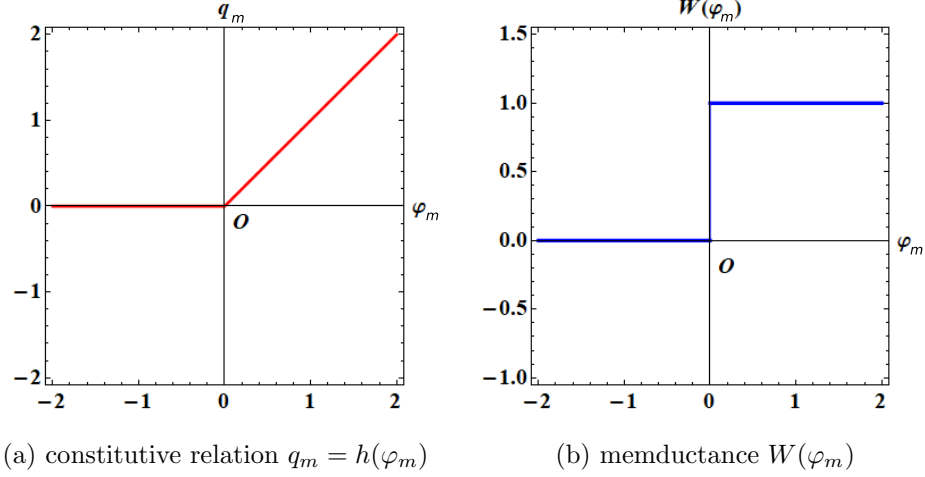


Figure 36: Constitutive relation and memductance of the flux-controlled memristor. The memristor switches “off” and “on” depending on the value of the flux φ_m .

(a) The constitutive relation of the memristor, which is given by $q_m = h(\varphi_m) \triangleq 0.5(|\varphi_m| + \varphi_m)$.

(b) Memductance $W(\varphi)$ of the memristor, which is defined by $W(\varphi_m) \triangleq \frac{dh(\varphi_m)}{d\varphi_m} = \mathfrak{s}[\varphi_m]$. Here, the symbol $\mathfrak{s}[z]$ denotes the *unit step* function, equal to 0 for $z < 0$ and 1 for $z \geq 0$.

The memristor CNNs in Figures 35 and 37 work as follows:

1. Normal procedure

Turn “off” the switch S_A in Figure 35. In this case, the output y_{ij} is *not* connected to the memristor, and the memristor CNN circuit works normally. The dynamics is given by Eq. (65).

2. Stored procedure

Turn “on” the switch S_A in Figure 35 during the period from t_0 to $t_0 + T$, where $0 < T \ll 1$. In this period, the output y_{ij} is connected to the memristor. The stored flux is given by

$$\varphi_m(T) = \int_{t_0}^{t_0+T} y_{ij}(t)(\tau) d\tau. \quad (120)$$

It is recast into the form

$$\frac{\varphi_m(T)}{T} = \frac{\int_{t_0}^{t_0+T} y_{ij}(t)(\tau) d\tau}{T}, \quad (121)$$

which is the *time average* of the output $y_{ij}(t)$.

Thus, $\varphi_m(T)$ is regarded as the time average of the output $y_{ij}(t)$ except for a scale factor of T .

3. Suspend procedure

Power off the memristor CNN in Figure 35 at $t = t_0 + T$. Then the computing process is suspended. The ideal memristor can retrieve stored information even after power off, since it is a *non-volatile* element. If the memristor is not ideal, for example, it has a parasitic capacitance as shown in Figure

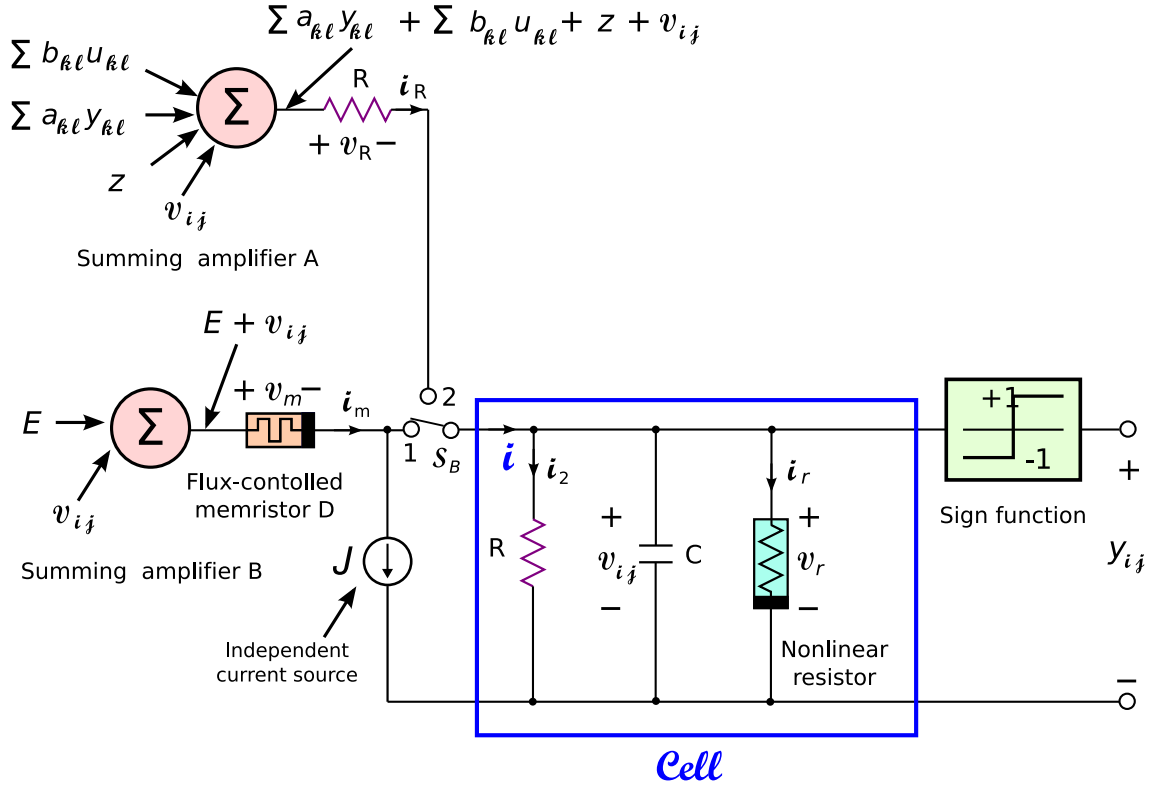


Figure 37: Circuit for recovering the previous average output, and for resuming the computation. At first, the switch S_B is set to the position 1 in order to recover the previous average output. Then, the switch S_B is set to the position 2 in order to resume the computation.

(1) Parameters: $E = 1$, $J = 0.5$, $R = 1$, $C = 1$.

(2) The $v - i$ characteristic of the nonlinear resistor (light blue) is given by $i_r = f_r(v_r) \triangleq -0.5 a (|v_r + 1| - |v_r - 1|)$, where a is a constant.

(3) The terminal currents and voltages of the memristor D satisfies $i_m = W(\varphi_m) v_m = \mathfrak{s}[\varphi_m] v_m$.

(4) The output voltage of the summing amplifier A is given by $\sum_{k, l \in N_{ij}, k \neq i, l \neq j} a_{kl} \text{sgn}(v_{kl}) + \sum_{k, l \in N_{ij}} b_{kl} u_{kl} + z + v_{ij}$.

(5) The above output voltage contains the voltage v_{ij} of the capacitor C (the last term).

(6) The above sum $\sum_{k, l \in N_{ij}, k \neq i, l \neq j} a_{kl} \text{sgn}(v_{kl})$ does not contain the term $a_{ij} \text{sgn}(v_{ij})$, ($k = i$, $l = j$).

(7) The output voltage of the summing amplifier B is equal to $E + v_{ij}$.

(8) The output y_{ij} and the state v_{ij} of each cell are related via the sign function (green): $y_{ij} = \text{sgn}(v_{ij})$.

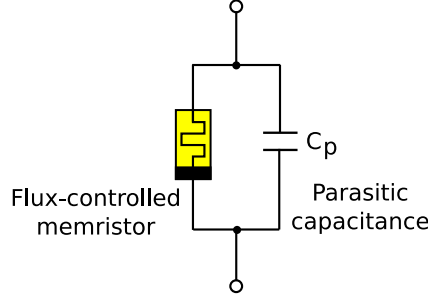


Figure 38: Parasitic capacitance C_p of the flux-controlled memristor.

38, then after long time power off, the flux of the memristor may decay via a parasitic capacitance [7]. We discuss its effect in Sec. 10.

4. Recovery procedure

In order to continue the process from the previous state, we use the circuit in Figure 37, where we use the memristor in Figure 35.

Let us first set the switch S_B to the position 1 at $t = t_1$. Then, the current i through the cell is given by

$$\begin{aligned}
 i(t) &= W(\varphi_m(t))E + J \\
 &= \mathfrak{s}[\varphi_m(t)] - 0.5 \\
 &= \begin{cases} 0.5 & \text{for } \varphi_m(t) \geq 0, \\ -0.5 & \text{for } \varphi_m(t) < 0, \end{cases}
 \end{aligned} \tag{122}$$

where $E = 1$, $J = 0.5$, and $\varphi_m(t)$ is defined by

$$\begin{aligned}
 \varphi_m(t) &= \int_{t_1}^t E d\tau + \varphi_m(T) \\
 &= E\Delta t + \varphi_m(T) = \Delta t + \varphi_m(T),
 \end{aligned} \tag{123}$$

where $0 < \Delta t \triangleq t - t_1$ and $E = 1$.

Assume that $0 < \Delta t < |\varphi_m(T)|$. Then we obtain

$$\text{sgn}(\varphi_m(t)) = \text{sgn}(\varphi_m(T)). \tag{124}$$

From Eq. (122), we obtain

$$i(t) = \begin{cases} 0.5 & \text{for } \varphi_m(T) \geq 0, \\ -0.5 & \text{for } \varphi_m(T) < 0. \end{cases} \tag{125}$$

Consider next the dynamics of the cell, which is given by

$$\begin{aligned}
 \frac{dv_{ij}}{dt} &= F(v_{ij}) \\
 &\triangleq -v_{ij} + 0.5a(|v_{ij} + 1| - |v_{ij} - 1|) + i(t).
 \end{aligned} \tag{126}$$

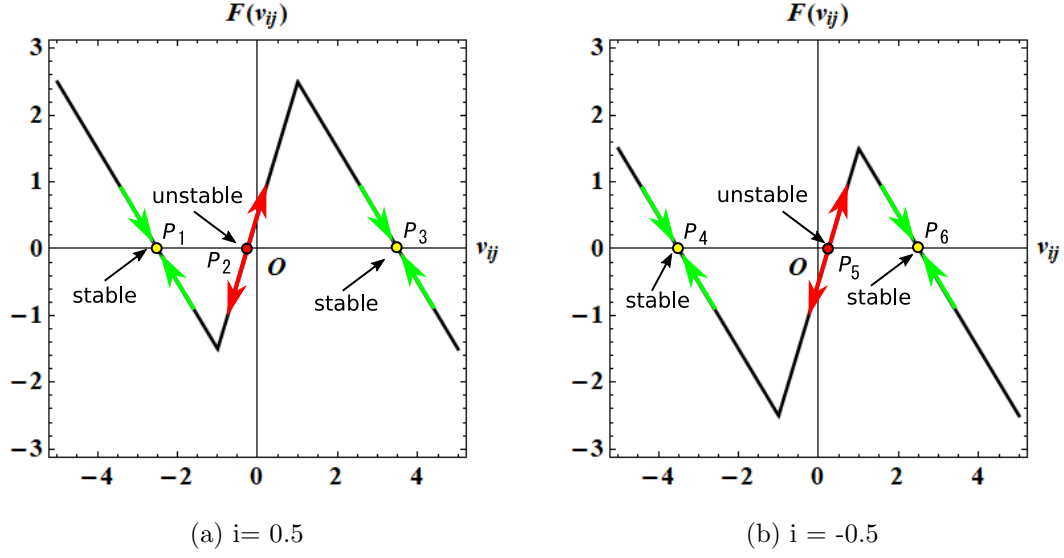


Figure 39: Driving-point plot of Eq. (126) with $a = 3$. Equation (126) has two stable equilibrium points (yellow), and one unstable equilibrium points (red). If $i = 0.5$, then $P_1 = -2.5$, $P_2 = -0.25$, $P_3 = 3.5$. If $i = -0.5$, then $P_4 = -3.5$, $P_5 = 0.25$, $P_6 = 2.5$.

We show the driving-point plot of Eq. (126) in Figure 39. Let us consider the case where $a = 3 > 1$. Then, Eq. (126) has two stable equilibrium points, and one unstable equilibrium points as shown in Figure 39. Furthermore, if $i(t) = 0.5$, then the equilibrium points are given by

$$P_1 = -2.5, P_2 = -0.25, P_3 = 3.5, \quad (127)$$

where the points P_1 and P_3 are stable, and the point P_2 is unstable. If $i(t) = -0.5$, then the equilibrium points are given by

$$P_4 = -3.5, P_5 = 0.25, P_6 = 2.5, \quad (128)$$

where the points P_4 and P_6 are stable, and the point P_5 is unstable.

The initial condition for Eq. (126) is given by $v_{ij}(t_1) = 0$, since the power of the system was turned off during the period of time from $t_0 + T$ to t_1 . From the driving-point plot in Figure 39, we obtain

$$\left. \begin{array}{l} \text{if } i(t) = 0.5 \text{ and } v_{ij}(t_1) = 0, \\ \text{then } v_{ij}(t) \rightarrow P_3 = 3.5 \text{ for } t \rightarrow \infty. \\ \text{if } i(t) = -0.5 \text{ and } v_{ij}(t_1) = 0, \\ \text{then } v_{ij}(t) \rightarrow P_4 = -3.5 \text{ for } t \rightarrow \infty. \end{array} \right\} \quad (129)$$

Here, the initial condition is given by $v_{ij}(t_1) = 0$.⁸ Since the solution $v_{ij}(t)$ of Eq. (126) for $t > t_1$ can *not* move across the unstable equilibrium point, we obtain

$$\left. \begin{array}{l} y_{ij}(t) = 1, \text{ if } i(t) = 0.5, \\ y_{ij}(t) = -1 \text{ if } i(t) = -0.5, \end{array} \right\} \quad (130)$$

where $y_{ij}(t) = \text{sgn}(v_{ij}(t))$. Furthermore, from Eqs. (125) and (130), we obtain

$$y_{ij}(t) = \text{sgn}(v_{ij}(t)) = \begin{cases} 1 & \text{if } \varphi_m(T) \geq 0, \\ -1 & \text{if } \varphi_m(T) < 0, \end{cases} \quad (131)$$

⁸Note that the power was turned off during the period of time from $t_0 + T$ to t_1 . Thus, $v_{ij}(t_1) = 0$.

where $\varphi_m(T)$ denotes the stored flux during the period from t_0 to $t_0 + T$, and it is the time average of the output $y_{ij}(t)$ except for a scale factor of T . We have just recovered the previous average output from $\varphi_m(T)$.⁹

5. Resume procedure

Set the switch S_B to the position 2. Then, the image processing starts again from the previous average output state. That is, we can resume the computation.

We show next two examples of the suspend and resume feature.

9.1 Hole-filling

Let us consider the *hole-filling template* [1, 8]

$$A = \begin{bmatrix} 0 & 1 & 0 \\ 1 & 3 & 1 \\ 0 & 1 & 0 \end{bmatrix}, \quad B = \begin{bmatrix} 0 & 0 & 0 \\ 0 & 4 & 0 \\ 0 & 0 & 0 \end{bmatrix}, \quad z = \boxed{-1}. \quad (132)$$

The initial condition for the state v_{ij} is equal 1, and the input u_{kl} is equal to a given binary image. The boundary condition is given by

$$v_{k^*l^*} = 0, \quad u_{k^*l^*} = 0, \quad (133)$$

where k^*l^* denotes boundary cells. This template can fill the interior of all closed contours in a binary image as shown in Figure 40.

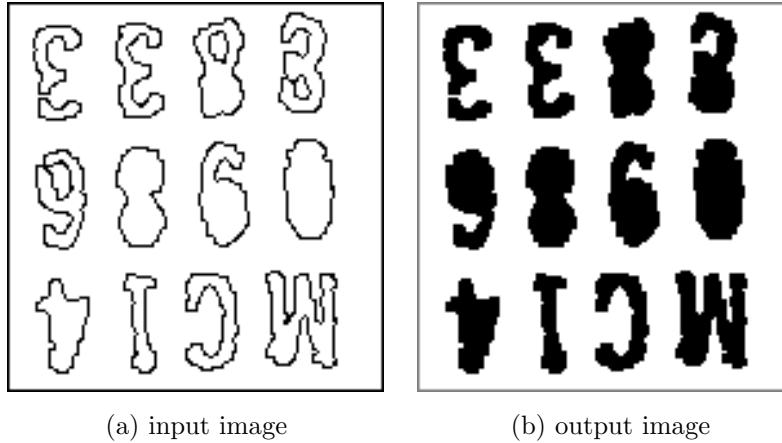


Figure 40: Input and output images for the hole-filling template (132). This template can fill the interior of all closed contours in a binary input image (left). Image size is 146×151 .

We show our detailed computer simulations in Figure 41. Observe that even if we turn off the power of the memristor CNN during the computation, it can resume from the previous average output state.

⁹We did not use $y_{ij}(t_0 + T)$, but $\varphi_m(T)$, where the system is turned off at $t = t_0 + T$.

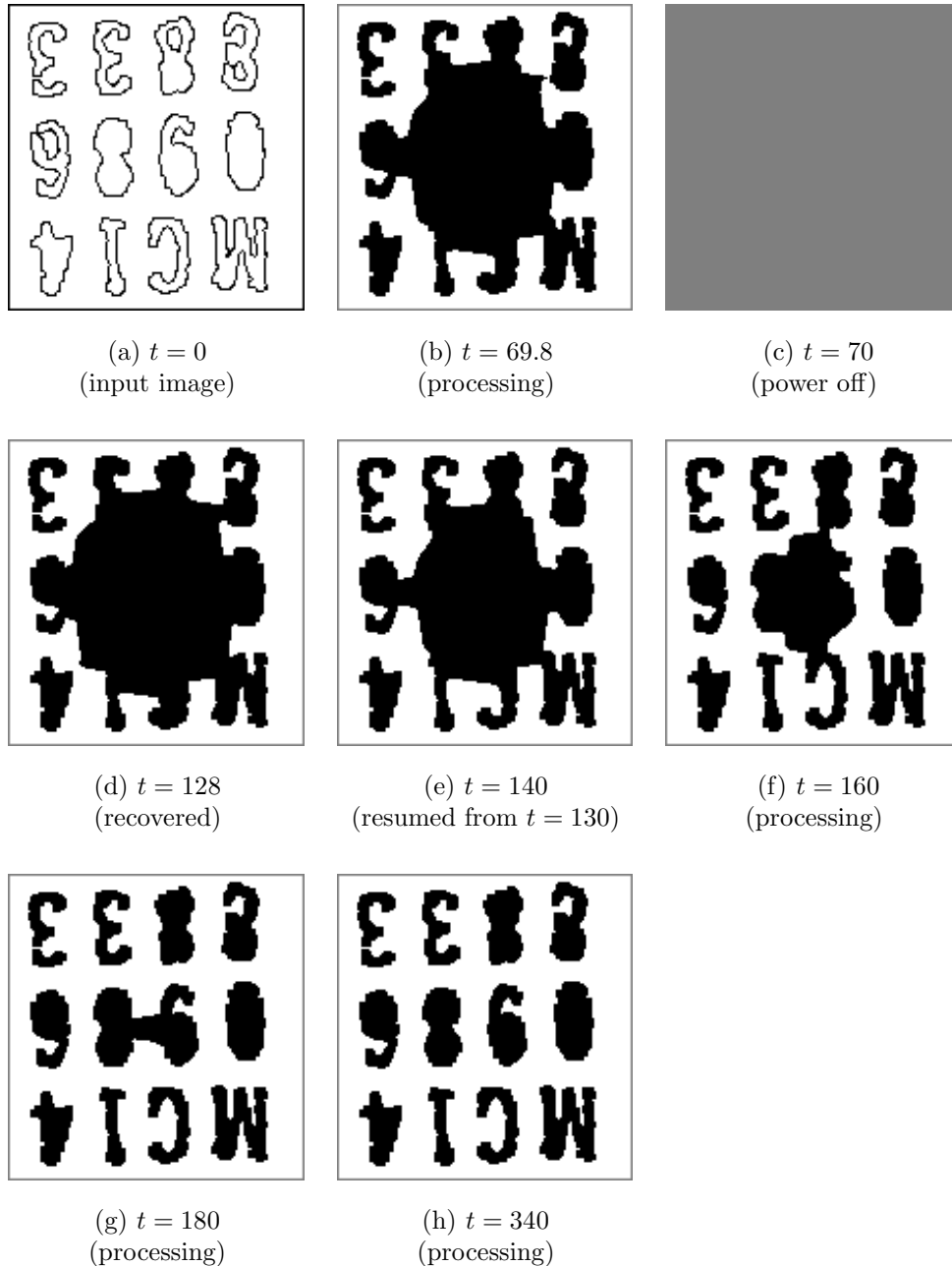


Figure 41: Suspend and resume feature for the hole-filling template (132).

(a) Input image (image size is 146×151).

(b) Processing image at $t = 69.8$. The switch S_A in Figure 35 is closed during the period $t \in [60, 70)$.

(c) Power off during the period $t \in [70, 120)$. In this period, the cell output $y_{ij} = 0$ (gray in pseudo-color).

(d) Recovered image at $t = 128$. The previous *average* output is recovered by setting the switch S_B in Figure 37 to the position 1. The recovering period is $t \in [120, 130)$.

(e)-(h) Processed images at time $t = 140, 160, 180, 340$, which are resumed from $t = 130$. In this period, the switch S_B in Figure 37 is set to the position 2. Observer that the memristor CNN can fill the interior of all closed contours in the binary input image, even if we power off the circuit in the middle of image processing.

9.2 Half-toning

Let us consider the *half-toning template* [1, 8]

$$\begin{aligned}
 A &= \begin{array}{|c|c|c|} \hline -0.07 & -0.1 & -0.07 \\ \hline -0.1 & 1.15 & -0.1 \\ \hline -0.07 & -0.1 & -0.07 \\ \hline \end{array}, \\
 B &= \begin{array}{|c|c|c|} \hline 0.07 & 0.1 & 0.07 \\ \hline 0.1 & 0.32 & 0.1 \\ \hline 0.07 & 0.1 & 0.07 \\ \hline \end{array}, \\
 z &= \boxed{0}.
 \end{aligned} \tag{134}$$

The initial condition for the state v_{ij} is equal to a given gray-scale image, and the input u_{kl} is also equal to a given gray-scale image. The boundary condition is given by

$$v_{k^*l^*} = 0, \quad u_{k^*l^*} = 0, \tag{135}$$

where k^*l^* denotes boundary cells. This template can transform a gray-scale image into a “half-tone” binary image. The binary image preserves the main features of the gray-scale image as shown in Figure 42.

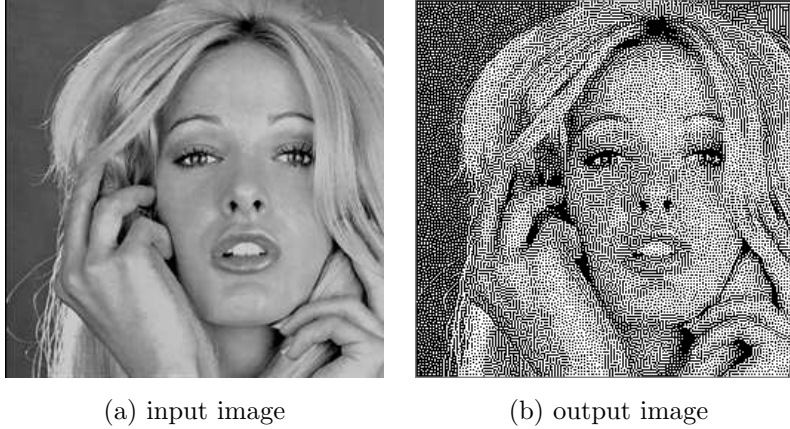


Figure 42: Input and output images for the half-toning template (132). This template can transform a gray-scale input image (left) into a “half-tone” binary image (right). The binary image preserves the main features of the gray-scale image. Image size is 256×256 .

Since $a = a_{0,0} = 1.15$, Eq. (126) has only one stable equilibrium points as shown in Figure 43. If $i(t) = 0.5$, then the equilibrium points are given by

$$Q_1 = 1.65. \tag{136}$$

If $i(t) = -0.5$, then the equilibrium points are given by

$$Q_2 = -1.65. \tag{137}$$

Thus, we obtain

$$\left. \begin{aligned}
 &\text{if } i(t) = 0.5 \text{ and } v_{ij}(t_1) = 0, \\
 &\text{then } v_{ij}(t) \rightarrow Q_1 = 1.65 \text{ for } t \rightarrow \infty. \\
 &\text{if } i(t) = -0.5 \text{ and } v_{ij}(t_1) = 0, \\
 &\text{then } v_{ij}(t) \rightarrow Q_2 = -1.65 \text{ for } t \rightarrow \infty.
 \end{aligned} \right\} \tag{138}$$

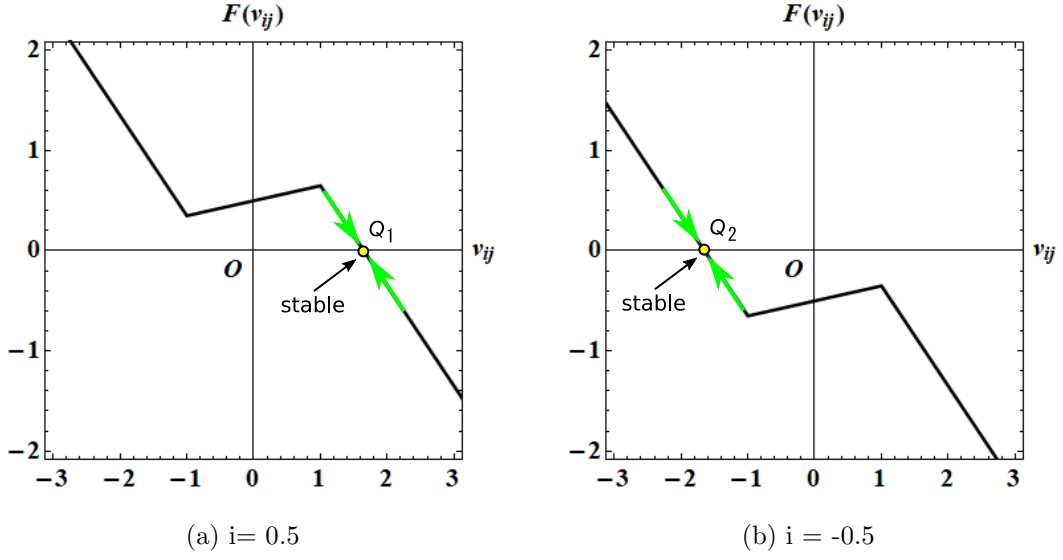


Figure 43: Driving-point plot of Eq. (126) with $a = 1.15$. Equation (126) has only one stable equilibrium points (yellow). Furthermore, if $i = 0.5$, then the stable equilibrium point is given by $Q_1 = 1.65$. If $i = -0.5$, then the stable equilibrium point is given by $Q_2 = -1.65$.

Here, the initial condition is given by $v_{ij}(t_1) = 0$.¹⁰ Since $y_{ij}(t) = \text{sgn}(v_{ij}(t))$, we obtain

$$\left. \begin{aligned} y_{ij}(t) &= 1, \text{ if } i(t) = 0.5, \\ y_{ij}(t) &= -1 \text{ if } i(t) = -0.5. \end{aligned} \right\} \quad (139)$$

Furthermore, from Eqs. (125) and (130), we obtain

$$y_{ij}(t) = \text{sgn}(v_{ij}(t)) = \begin{cases} 1 & \text{if } \varphi_m(T) \geq 0, \\ -1 & \text{if } \varphi_m(T) < 0, \end{cases} \quad (140)$$

where $\varphi_m(T)$ denote the stored flux during the period from t_0 to $t_0 + T$, and $\varphi_m(T)$ is regarded as the time average of the output $y_{ij}(t)$. Thus, we obtained the same result as that for $a = 3$ (see Eq. (131)).

We show next our detailed computer simulations in Figure 44. Observe that even if we turn off the power of the memristor CNN during the computation, it can resume from the previous average output state. Thus, we obtain the following result:

Assume $a_{00} > 1$. Then the memristor CNN has the suspend and resume feature, if we use the circuits in Figures 35 and 37.

¹⁰Note that the power was turned off during the period of time from $t_0 + T$ to t_1 . Thus, $v_{ij}(t_1) = 0$.

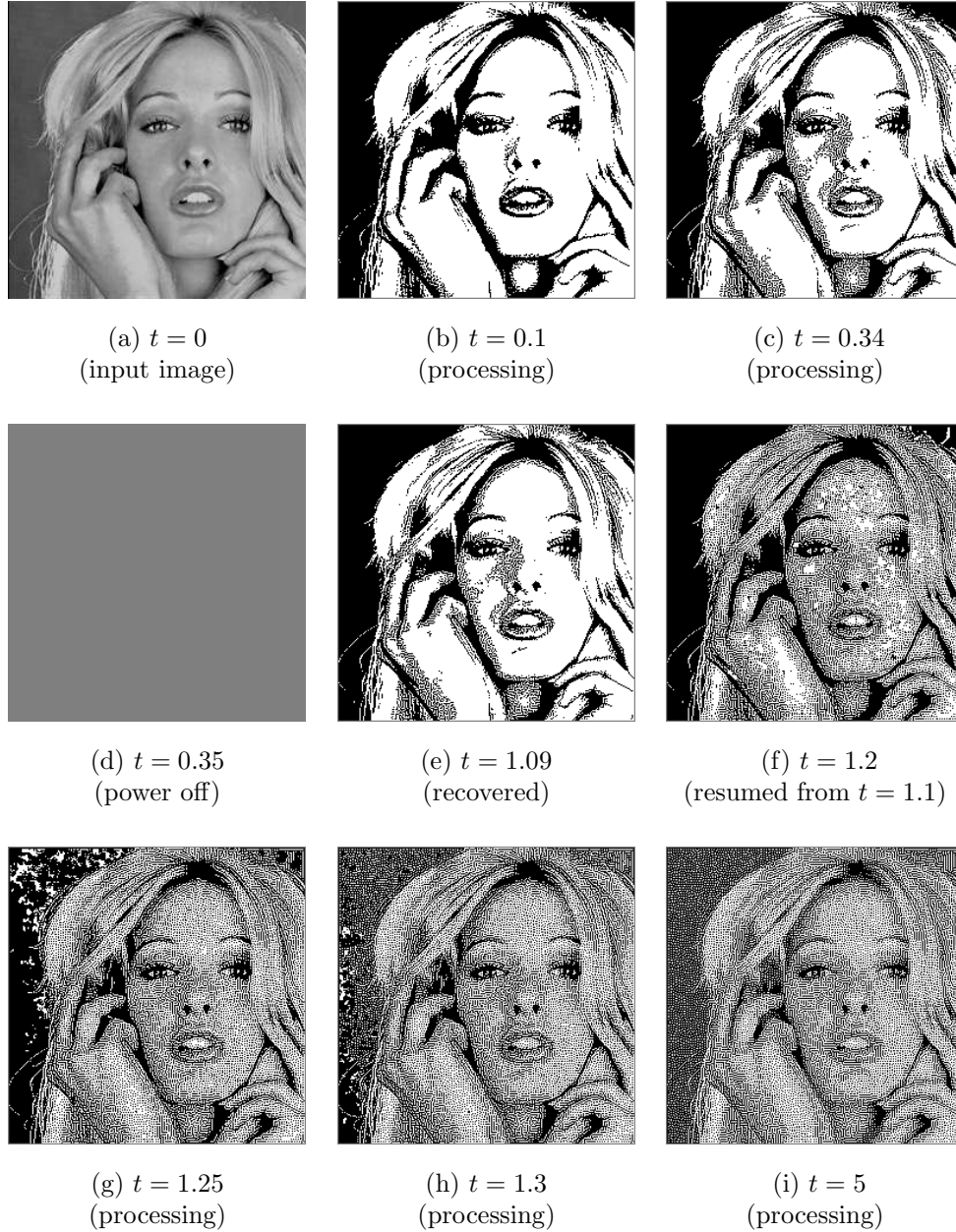


Figure 44: Suspend and resume feature for the half-toning template (134).

(a) Input image (image size is 256×256).

(b) Processing image at $t = 0.1$.

(c) Processing image at $t = 0.34$. Note that the switch S_A in Figure 35 is closed during the period $t \in [0.35, 0.6)$.

(c) Power off during the period $t \in [0.35, 1)$. In this period, the cell output $y_{ij} = 0$ (gray in pseudo-color).

(d) Recovered image at $t = 1.09$. The previous average output is recovered by setting the switch S_B in Figure 37 to the position 1. The recovering period is $t \in [1, 1.1)$.

(f)-(i) Processed images at time $t = 1.2, 1.25, 1.3, 2, 5$, which are resumed from time $t = 1.1$. In this period, the switch S_B in Figure 37 is set to the position 2. Observer that the memristor CNN can transform the recovered image into the half-tone binary image, even if we power off the circuit in the middle of image processing.

9.3 Long-term and short-term memories

In our brain’s system, a *long-term memory* is a storage system for storing and retrieving information. A *short-term memory* is the *short-time* storage system that keeps something in mind before transferring it to a long-term memory.

Consider the circuit in Figure 35. Thus, if the switch S_A in Figure 35 is “off”, then the output is hold only when the power is turned on. In this case, the circuit is regarded as a *short-term memory circuit*. If the switch S_A is “on”, then the time average of the output is stored in the memristor, and we can retrieve it, even if the power is turned off. That is, the ideal memristor can retrieve stored information even after power off, since it is a *non-volatile* element. In this case, the circuit becomes a *long-term memory circuit*. Thus, we conclude as follow:

The memristor CNN has functions of the *short-term* and *long-term* memories, if we use the circuits in Figure 35.

10 Effect of Flux Decay of Memristors

A certain degree of decay of the flux or the charge is inevitable in physical devices. For example, the flux of the memristor may decay via a parasitic capacitance after long time power off [7].

Let us assume that the flux φ_m decays to small value ϵ without change of sign. Then, the memductance $W(\varphi_m)$ satisfies

$$W(\varphi_m)\Big|_{\varphi_m=\epsilon} = W(\epsilon) = \mathfrak{s}[\epsilon] = \begin{cases} 1 & \text{if } \epsilon > 0, \\ 0 & \text{if } \epsilon < 0, \end{cases} \quad (141)$$

where $0 < |\epsilon| \ll 1$. The current i through the cell in Figure 37 is given by

$$\begin{aligned} i(t) &= W(\epsilon)E + J \\ &= \mathfrak{s}[\epsilon] - 0.5 \\ &= \begin{cases} 0.5 & \text{if } \epsilon > 0, \\ -0.5 & \text{if } \epsilon < 0. \end{cases} \end{aligned} \quad (142)$$

where $E = 1$, $J = 0.5$. From Eq. (130), we obtain

$$y_{ij}(t) = \begin{cases} 1 & \text{if } \epsilon > 0, \\ -1 & \text{if } -\epsilon < 0. \end{cases} \quad (143)$$

Thus, the output of the cell does not change even if the flux decays to small value. Note that the output $y_{ij}(t)$ depends on only the sign of ϵ , but it does not depend on its value. Thus, we can choose that $|\epsilon| = 0.001$ for the computer simulation.

We show our computer simulations in Figures 45 and 46, where we assume that the flux of the 50 percent of memristors decays to small value without change of sign after power off. Observe that the memristor CNN defined by Figures 35 and 37 works well.

The interesting thing is that if the flux of only the “1 percent” of memristors decay to small value with *change of sign*, then the hole-filling template does *not* work, as shown in Figure 47. Thus, the suspend and resume feature does not work if the change of sign occurs by memristor failures or parasitic elements. In this case, some error-correcting mechanisms should be used. However, the half-toning template works well even if the flux of “all” memristors decay to small value with *change of sign*, as shown in Figure 48. In this case, the output image for the half-toning template does not depend on the initial condition. Thus, we conclude as follow:

Assume $a_{00} > 1$. Then the memristor CNN defined by Figures 35 and 37 has the suspend and resume feature, even if the flux of the memristors decays to a small (but not too small) value, without change of sign, after power off.

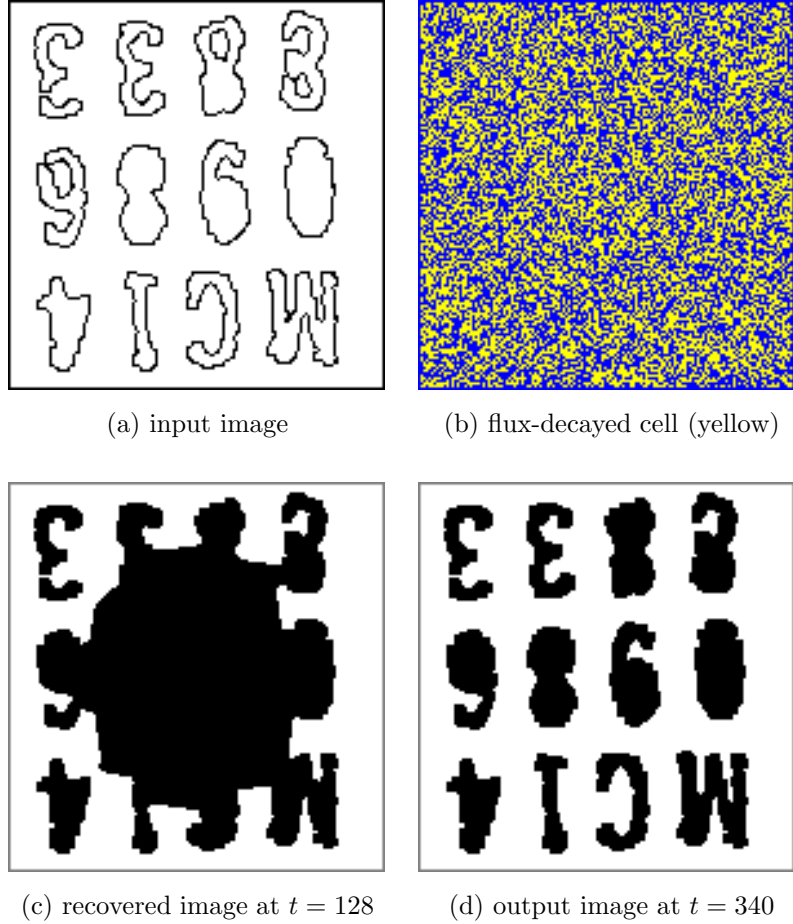


Figure 45: Suspend and resume feature for the hole-filling template (132) under the condition that the flux of the 50 percent of memristors decays to small value *without change of sign*.

(a) Input binary image (image size is 146×151).

(b) After power off (during the period $t \in [70, 120)$), we assume that the flux of the 50 percent of memristors decays to small value *without change of sign* by parasitic capacitances. The flux-decayed cells are colored in yellow. Other cells are colored in blue. The cell size is 146×151 , since the input image size is 146×151 .

(c) Recovered image at $t = 128$.

(d) Output image at $t = 340$. Observe that the memristor CNN defined by Figures 35 and 37 works well even if the flux of the 50 percent of memristors decays to sufficiently small value.

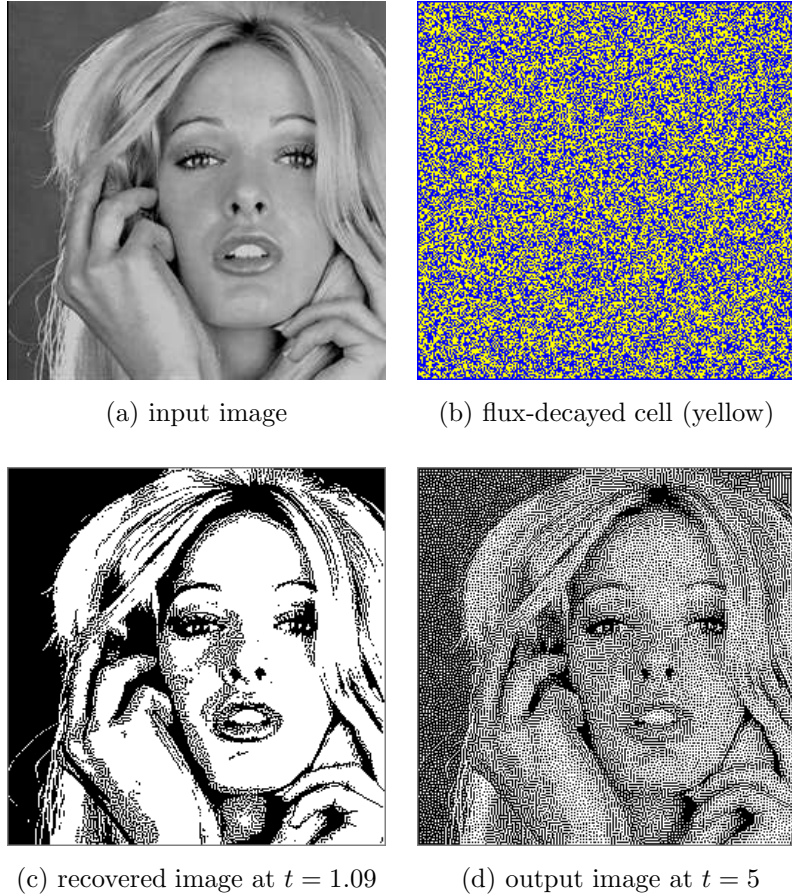


Figure 46: Suspend and resume feature for for the half-toning template (134) under the condition that the flux of the 50 percent of memristors decays to small value *without change of sign*.

(a) Input gray-scale image (image size is 256×256).

(b) After power off at $t = 0.35$, we assume that the flux of the 50 percent of memristors decays to small value *without change of sign* by parasitic capacitances. The flux-decayed cells are colored in yellow. Other cells are colored in blue. The cell size is 256×256 , since the input image size is 256×256 .

(c) Recovered image at $t = 1.09$.

(d) Output image at $t = 5$. Observe that the memristor CNN defined by Figures 35 and 37 works well even if the flux of the 50 percent of memristors decays to sufficiently small value.

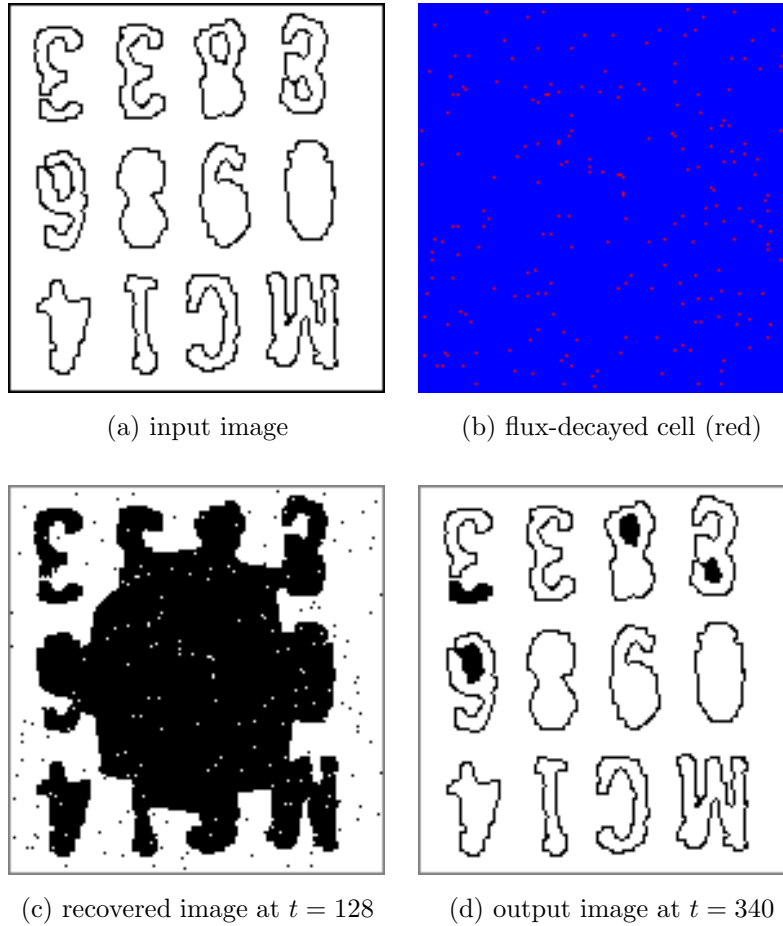


Figure 47: Suspend and resume feature for the hole-filling template (132) under the condition that the flux of the 1 percent of memristors decays to small value *with change of sign*.

(a) Input binary image (image size is 146×151).

(b) After power off at $t = 70$, we assume that the flux of the 1 percent of memristors decays to small value *with change of sign*. The flux-decayed cells are colored in red, and the other cells are colored in blue. The cell size is 146×151 , since the input image size is 146×151 .

(c) The recovered image at $t = 128$.

(d) Output image at $t = 340$. Observe that if the flux of the 1 percent of memristors decays to small value *with change of sign*, then the hole-filling template (132) does *not* work well.

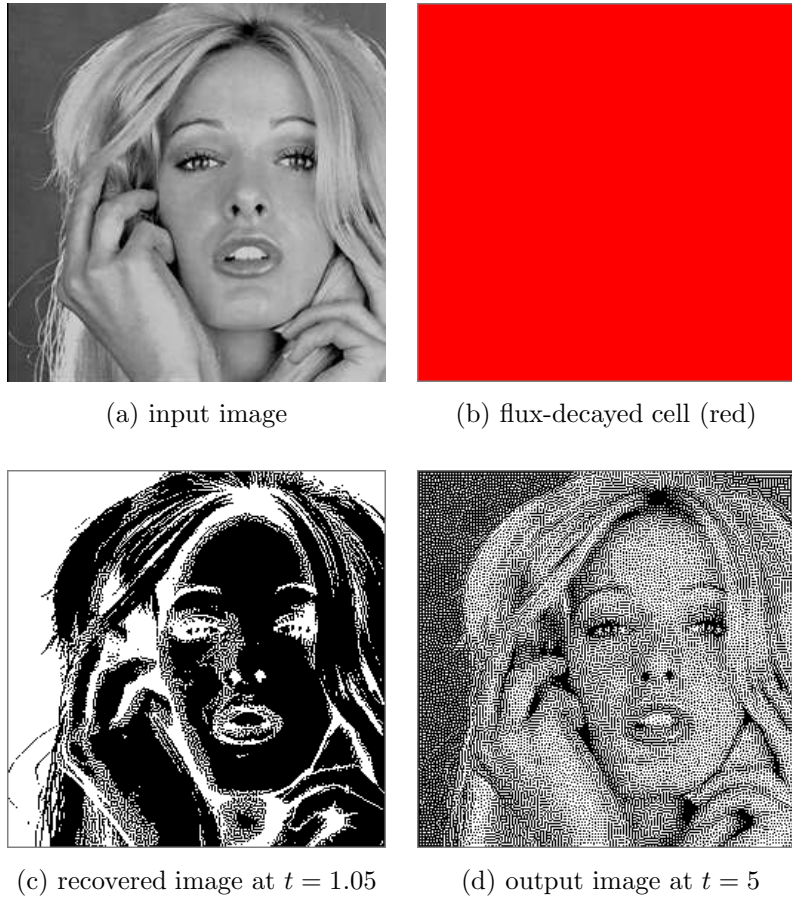


Figure 48: Suspend and resume feature for for the half-toning template (134) under the condition that the flux of *all* memristors decays to small value *with change of sign*.

(a) Input gray-scale image (image size is 256×256).

(b) After power off at $t = 0.35$, we assume that the flux of “*all*” memristors decays to small value *with change of sign*. The flux-decayed cells are colored in red. In this case, all cells are colored in red. The cell size is 256×256 , since the input image size is 256×256 .

(c) Recovered image at $t = 1.09$.

(d) Output image at $t = 5$. Observe that the half-toning template (134) works well, even if the flux of *all* memristors decays to sufficiently small value *with change of sign*.

11 Reset of Memristors

Before a new programming, we should reset the memristor to its zero state. A capacitor can simply be discharged by shorting its terminals (a wire has a negligibly small resistance). However, in order reset the flux of the memristor, we have to supply the *reversed* input signal, which was used in the previous programming. If the flux-controlled memristor is *ideal* and *passive*, then we can reset the memristor to its zero state by connecting a small capacitor to the memristor in parallel [7].

12 Two-dimensional Waves

In this section, we show that the memristor CNN can exhibit interesting two-dimensional waves. Consider the memristor CNN circuit in Fig. 49. We connected the inductor L in parallel with the capacitor C . In this case, the dynamics of the memristor CNN is given by

$$\begin{aligned}
 & \text{Dynamics of the memristor CNN} \\
 & C \frac{dv_{ij}}{dt} = i_{ij} - v_{ij} + 0.5 a (|v_{ij} + 1| - |v_{ij} - 1|) + W(\varphi_m) v_m, \\
 & L \frac{di_{ij}}{dt} = -v_{ij} \\
 & (i, j) \in \{1, \dots, M\} \times \{1, \dots, N\},
 \end{aligned} \tag{144}$$

where $L = C = 1$. The terminal currents and voltages of the flux-controlled memristor D (yellow) satisfies $i_m = W(\varphi_m) v_m$. Here, the memductance $W(\varphi_m)$ is defined by

$$\begin{aligned}
 W(\varphi_m) &= \alpha \mathfrak{s}[\varphi_m - a] - \beta \mathfrak{s}[\varphi_m - b] \\
 &= \left\{ \begin{array}{ll} \alpha & \text{for } -a \leq \varphi_m < a, \\ (\alpha - \beta) & \text{for } \varphi_m < -b \text{ and } b \leq \varphi_m, \end{array} \right\}
 \end{aligned} \tag{145}$$

where $\varphi_m(t) = \int_{-\infty}^t v_m(\tau) d\tau$, α , β , a , and b are parameters, and the symbol $\mathfrak{s}[z]$ denotes the *unit step* function, equal to 0 for $z < 0$ and 1 for $z \geq 0$, and $0 < a < b$.

Let us consider the *hole-filling template* [1, 8] again

$$A = \begin{bmatrix} 0 & 1 & 0 \\ 1 & 3 & 1 \\ 0 & 1 & 0 \end{bmatrix}, \quad B = \begin{bmatrix} 0 & 0 & 0 \\ 0 & 4 & 0 \\ 0 & 0 & 0 \end{bmatrix}, \quad z = \boxed{-1}. \tag{146}$$

The initial condition for the state v_{ij} and the input u_{kl} are equal to a given binary image. The boundary condition is given by

$$v_{k^*l^*} = 0, \quad u_{k^*l^*} = 0, \tag{147}$$

where k^*l^* denotes boundary cells. If we adjust the parameters α , β , a , and b , then the memristor CNN (144) can exhibit many interesting two-dimensional waves, as shown in Fig. 50.

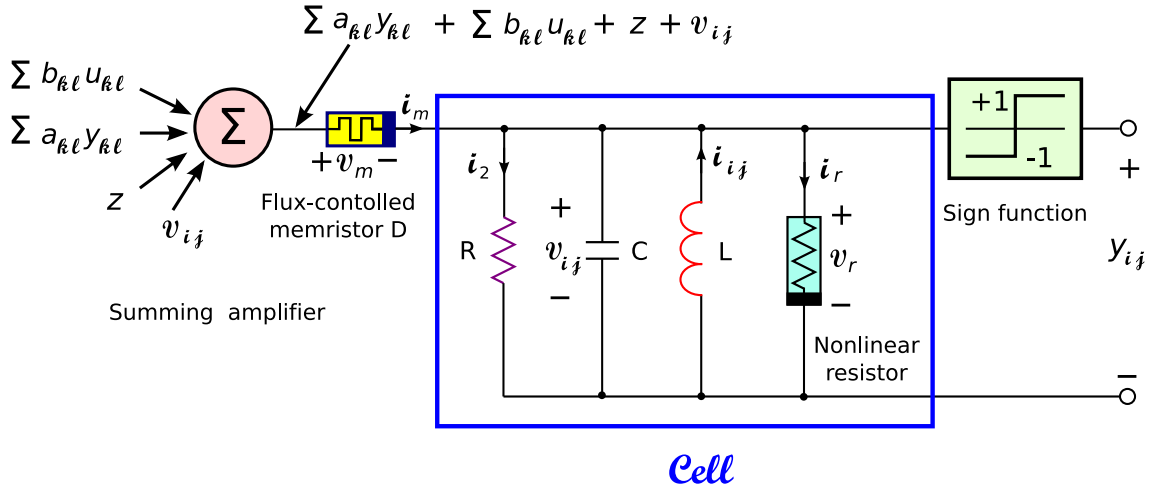


Figure 49: Memristor CNN circuit which can exhibit two-dimensional waves. We connected the inductor L (red) in parallel with the capacitor C .

(1) Parameters: $R = 1$, $C = 1$, $L = 1$.

(2) The $v - i$ characteristic of the nonlinear resistor (light blue) is given by $i_r = f_r(v_r) \triangleq -0.5 a (|v_r + 1| - |v_r - 1|)$, where a is a constant.

(3) The terminal currents and voltages of the flux-controlled memristor D (yellow) satisfies $i_m = W(\varphi_m) v_m$, where $W(\varphi_m)$ is the memductance defined by Eq. (refleqn: wave-W).

(4) The output voltage of the summing amplifier (pink) is given by
$$\sum_{k, l \in N_{ij}, k \neq i, l \neq j} a_{kl} \operatorname{sgn}(v_{kl}) +$$

$$\sum_{k, l \in N_{ij}} b_{kl} u_{kl} + z + v_{ij}.$$

(5) The above output voltage contains the voltage v_{ij} of the capacitor C (the last term).

(6) The above sum
$$\sum_{k, l \in N_{ij}, k \neq i, l \neq j} a_{kl} \operatorname{sgn}(v_{kl})$$
 does *not* contain the term $a_{ij} \operatorname{sgn}(v_{ij})$ ($k = i$, $l = j$).

(7) The output y_{ij} and the state v_{ij} of each cell are related via the sign function (green): $y_{ij} = \operatorname{sgn}(v_{ij})$.



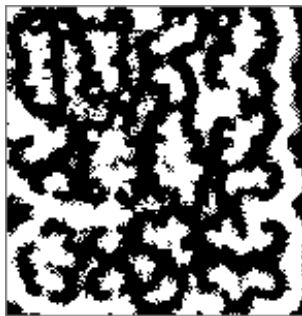
(a) input image



(b) $\alpha = 1, \beta = 1, a = 0.5, b = 4000$



(c) $\alpha = 1, \beta = 1, a = 1, b = 5000$



(d) $\alpha = 1, \beta = 1, a = 2, b = 5000$



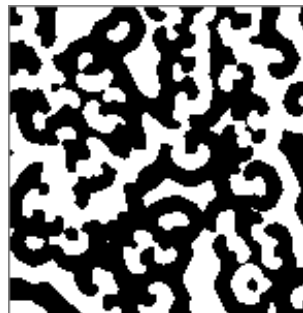
(e) $\alpha = 1, \beta = 1, a = 2.5, b = 5000$



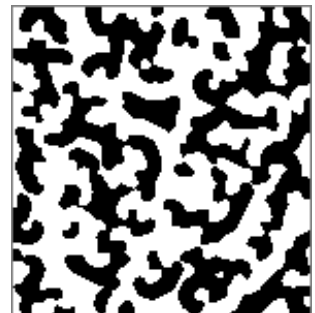
(f) $\alpha = -1, \beta = 2, a = 05, b = 35$



(g) $\alpha = -1, \beta = 2, a = 05, b = 50$



(h) $\alpha = -1, \beta = 2, a = 05, b = 2000$



(i) $\alpha = -1, \beta = 2, a = 05, b = 3000$

Figure 50: Two-dimensional waves, which is generated by the hole-filling template. (a) input image. (b)-(i) two-dimensional waves at $t = 2000$.

13 Conclusion

We have shown that the flux-controlled memristors cannot respond to the sinusoidal voltage source quickly. Furthermore, these memristors have the refractory period after switch “on”. We have shown that the memristor-coupled two-cell CNN can exhibit chaotic behavior. We have also proposed the memristor CNN, which can hold the output image, even if even if all cells are disconnected and no signal is supplied to the cell after a certain point of time, by memristor’s switching behavior. We have next shown that even if we turn off the power of the memristor CNN during the computation, it can resume from the previous average output state. That is, the memristor CNN has the suspend and resume feature. Furthermore, the memristor CNN has functions of the short-term and long-term memories. Finally, we have shown that the memristor CNN can exhibit the interesting two-dimensional waves, if an inductor is connected to each memristor CNN cell. In this paper, we used the Euler method for solving the differential equations. In order to get more accurate results, we may need high accuracy numerical methods, for example, the Runge-Kutta method.

References

- [1] Chua, L. O. (1998) *CNN: A Paradigm for Complexity* (World Scientific, Singapore).
- [2] Chua, L. O. and Roska, T. (2002) *Cellular neural networks and visual computing* (Cambridge University Press, Cambridge), 2002.
- [3] Itoh, M. and Chua, L.O. (2003) Designing CNN genes. *Int. J. Bifurcation and Chaos*, **13**(10), 2739-2824.
- [4] Itoh, M. and Chua, L.O. (2009) Memristor cellular automata and memristor discrete-time cellular neural networks. *Int. J. Bifurcation and Chaos*, **19**(11), 3605-3656.
- [5] Chua, L. O. (1971) Memristor–The missing circuit element. *IEEE Transactions on Circuit Theory*, **CT-18** (5), 507-519.
- [6] Chua, L. O. and Kang, S. M. (1976) Memristive devices and systems. *Proc. IEEE*, **64**(2), 209-223.
- [7] Itoh M. and Chua L. O. (2016) Parasitic effects on memristor dynamics. *Int. J. Bifurcation and Chaos*, **26**(6), 1630014-1-55.
- [8] Roska, T., Kék, L., Nemes, L., and Zarándy, Á. (1997) CNN software library (templates and algorithms). version 7.0 (DNS-1-1997). Analogical and Neural Computing Laboratory, Computer Automation Institute, Hungarian Academy of Sciences, Budapest, Hungary.